

A Risk Based Paradigm and Model for Unmanned Aerial Systems in the National Airspace

Christopher W. Lum* and Blake Waggoner†

Autonomous Flight Systems Laboratory

University of Washington, Seattle, WA, 98195, USA

A major focus of current unmanned systems operations is assessing the inherent risk associated with a mission. Efforts to integrate unmanned systems into the national airspace require manufacturers be able to calculate the risk of a mission in terms of human safety. Threats to human safety from midair collisions and ground strikes are the focus of the risk model. The project's intent is to assist in determining applications that leverage the strengths of current unmanned aircraft technology while mitigating the weaknesses so as to meet or exceed the safety and economic viability of manned aircraft. The validity of the risk model is demonstrated by comparison to historical data when available. The intended use of the tool is discussed and risk assessments are presented for several example scenarios. Resources for gathering the required information are surveyed and material is developed to aid a general audience in performing a risk assessment.

Nomenclature

A_b	Average building area (km ²)
ADS-B	Automatic Dependent Surveillance-Broadcast
A_{LHb}, A_{LHP}	Lethal area for buildings and pedestrians in a horizontal crash (due to system failure) (km ²)
A_{LVb}, A_{LVP}	Lethal area for buildings and pedestrians in a vertical crash (due to midair collision) (km ²)
A_{ops}	Operating area size (km ²)
C_{midair}	Rate of aircraft crashes due to midair (transient & in-flight) collisions (crashes/hour)
C2	Command and Control
D_{bldg}	Expected number of fatalities when a UA collides with a building
D_{ped}	Expected number of fatalities when a UA collides with a pedestrian (in range [0, 1])
F_{fat}	Fatalities per flight hour
$F_{fat,p}$	Fatalities due to system failures (fatalities/hour)
$F_{fat,midair}$	Fatalities due to midair collisions (fatalities/hour)
F_{ped}	Collision rate of UA fleet with pedestrians per hour (collisions/hour)
$F_{bldg,midair}$	Collision rate with buildings due to midair collision (collision/hour)
$F_{bldg,p}$	Collision rate with buildings due to system failure (collision/hour)
$F_{ped,midair}$	Collision rate with pedestrians due to midair collision (collision/hour)
$F_{ped,p}$	Collision rate with pedestrians due to system failure (collision/hour)
F_{bldg}	Collision rate of UA fleet with buildings per hour (collisions/hour)
F_{fleet}	Collision rate of UA fleet of other UA within fleet per flight hour (collisions/hour)
$\hat{F}_{transient}$	Collision rate of a single UA w/o avoidance & stationary transient AC (collisions/flight-hour)
$\tilde{F}_{transient}$	Collision rate of UA fleet w/o avoidance & moving transient AC (collisions/hour)
$F_{transient}$	Collision rate of UA fleet with transient AC per hour (collisions/hour)
H	Total aircraft flight hours recorded in historical data (aircraft-hours)
H_b	Average building height (km)
H_p	Average pedestrian height (km)

*Research Scientist, Dept. of Aeronautics and Astronautics, lum@u.washington.edu

†Research Assistant, Dept. of Aeronautics and Astronautics, bjwaggs@u.washington.edu

I_{fat}	Insurance liability per fatality (dollars/fatality)
L_{ua}	Length of UA (km)
M	Cost to insure the operation per hour (dollars/hour)
M_L	Mission length (hours)
N_{ua}	Number of UA in fleet
NAS	National Airspace
P_o	Average number of passengers on a transient aircraft (people/AC)
R_p	Radius of a pedestrian (km)
SAA	Sense and Avoid
TBO	Trajectory Based Operations
UA/UAS	Unmanned Aircraft/Unmanned Aerial System
V_o and V_{ua}	Velocity of transient aircraft and UA (km/hour)
w_o	Average width of buildings (km)
w_{ua}	Wingspan of UA (km)
z_{max}, z_{min}	Maximum and minimum altitude of operating area (km)
α, α_H	Number of mission collisions predicted by model and historically recorded, respectively
γ	Best glide angle of UA (radians)
ρ_o, ρ_{ua}	Density of transient AC and UA, respectively (AC/km ³)
ϕ_{col}	Instantaneous collision area (km ²)
ϕ_o, ϕ_{ua}	Frontal area of transient aircraft and UA (km ²)
ϵ_o	Ability of transient AC to avoid collisions with UA (in range [0, 1])
$\epsilon_{ua/o}$	Ability of UA to avoid collisions with transient AC (in range [0, 1])
$\epsilon_{ua/ua}$	Ability of UA to avoid collisions with other UA in fleet (in range [0, 1])
η_{ops}	Volume of entire operating space of mission (km ³)
η_{fleet}	Volume of only operating space where UA fleet exists (km ³)
λ	UAS midair failure rate for a single AC (failures/hour)
σ_b, σ_p	building and pedestrian densities (items/km ²)

I. Introduction

The past several decades have seen significant advances in unmanned aircraft system (UAS) technology. In the last 10 years there has been a corresponding increase in their use by military organizations around the world. The adoption of UAS for non-military purposes, however, has been quite slow. This trend has been especially true in the U.S. where concerns over their safe integration into the national airspace system (NAS) have often stifled efforts to employ UAS for the purposes of private industry, academia, and domestic government applications. While the complete integration of UAS is still years away, there are currently many practical uses for unmanned aircraft whose associated risk is equal to or better than that of manned aircraft. Reliable and realistic methods of evaluating risk must be developed in order to allow further development and use of UAS while ensuring public safety. This paper documents the development of a simplified model to assess and predict the risk associated with a given UAS operation. This tool is intended to be useful for determining UAS applications that are viable from the related perspectives of risk to human safety.

Anno¹ was one of the first to address parts of this issue by modeling mid-air collisions using random collision theory and comparing results to historical data. More recent and similar risk-based approach to analyzing the safety of UAS operations was taken by Burke² at North Carolina State University in the development of the System Level Airworthiness Tool (SLAT). The author also chose to focus on the expected number of fatalities per flight hour as the primary safety metric. The actual risk assessment examines the UAS in more detail at the system level in order to define a more complete approach to certification.

Additional references and prior work are presented in the context of the federal UAS policy in Section II. This section serves as motivation by looking at current US policy relevant to UAS operations. Section III then describes some of the framework used to develop the overall risk model which is then presented in Section IV. Results and validation of the proposed model are shown in Section V before exploring some detailed examples of the tool applied to actual missions in Section VI. Finally, Section VII presents conclusions and future directions of research.

II. Current UAS Policy

Without a thorough understanding of the risks involved, regulations on the flight of UAS in US airspace have thus far been highly prohibitive. Policy was set forth in a September, 2005 Federal Aviation Administration (FAA) memorandum,³ clarified in a 2006 notice,⁴ and replaced in March 2008 by the Interim Operational Approval Guidance.⁵ Currently, the only avenue to receive approval of civil (i.e. commercial, academia) UAS operation is through a special experimental airworthiness certificate. The special certificate is subject to operational limitations (e.g. line of sight operation, daylight hours, etc.) and is only issued “for the purposes of research and development, crew training, or market survey.” The procedure and guidelines for issuing a special experimental certificate are detailed by the FAA.⁶

A second avenue, a certificate of authorization (COA), was closed to civil applications in 2005 by FAA memorandum AFS-400³ but is still used for public (i.e. government/military) requests after the vehicle has been deemed airworthy by the FAA or DoD. A category that a minority of UAS may fall under is model aircraft⁷ (strictly non-business related). Other documents of interests include NATO’s UAV Systems Airworthiness Requirements⁸ and the European Aviation Safety Agency’s (EASA) statement on Airworthiness Certification of Unmanned Aircraft Systems.⁹

UAS policy is currently being reviewed to develop a long-term approach to a fluid integration of UAS into the NAS. Several components of the NextGen Air Transportation System (ATS) should help facilitate this process in the coming years.¹⁰ NextGen refers to the next generation of the NAS being incrementally implemented over the course of several years, with current mid-term goals set through 2018. Two key NextGen technologies that have the greatest potential to impact UAS integration are Automatic Dependent Surveillance-Broadcast (ADS-B) and 4D Trajectory Based Operations (TBO).^{11,12} The FAA’s perspective on UAS has been supportive but cautious as indicated by the following excerpt,³

“The FAA supports UA flight activities that can demonstrate that the proposed operations can be conducted at an acceptable level of safety. AFS intends to approve COA applications... [if] a collision with another aircraft...is extremely improbable...[and] injury to persons or property along the flight path is extremely improbable. Acceptable system safety studies must include a hazard analysis, risk assessment, and other appropriate documentation that support the ‘extremely improbable’ determination.”

A. Motivation

It is generally perceived that there are a number of obstacles to the full integration of UAS into the NAS. The most pressing technological challenges are “sense and avoid” (SAA) capability and command and control (C2) link liabilities.¹² Sense and avoid refers to the capability of an autonomous vehicle to detect objects, both stationary and mobile, that do not broadcast their position, which are in the vehicle’s path (or otherwise on a collision course) and, if necessary, alter the vehicle’s course to avoid a collision. Since the pilot of a UAS is not able to provide the “see and avoid” ability of an onboard pilot, the development of reliable SAA technology is believed to be essential for UAS to gain full airspace access. Significant work has been done both in R&D of SAA technologies and in establishing qualifications for an acceptable SAA system.¹³

Although most UA^a will have low-level autonomy, a reliable communication link between the UA and the pilot is necessary for high-level control (navigation, tasking, air traffic control, etc.). In addition to improving the C2 link reliability, protocols must be developed to ensure safe and predictable behavior in the case of a lost-link. There is also much work to be done on the policy front. Guidelines are needed on airworthiness, crew training, operational protocols and how UAS will fit into the current and NextGen airspace structures.

Thoroughly addressing all of these issues, so that UAS may be routinely and safely incorporated throughout the NAS, will take years. In the meantime, standards and tools need to be developed that will, “enable the widest range of activity that can be safely conducted within the shortest rulemaking timeframe” (ASTM F38 Committee). Until new technologies are developed and a new system is in place, UAS operation approvals will continue to require mission specific risk assessments.

The purpose of the risk assessment tool presented in this paper is two-fold. First, it seeks to provide UAS operators and airspace regulators with a simplified and trustworthy method of evaluating the safety of proposed UAS operations. Tools are needed that provide UAS operators with “documentation that support

^aUA is used to refer only to the aircraft, whereas UAS refers to the whole system inclusive of all ground-based equipment and any communication links.

the ‘extremely improbable’ determination,” since it is an essential part of the current approval process. The availability of a tool to assess the risk of particular proposed UAS operation should make the process of obtaining approval more efficient and manageable.

The second objective is that the results of risk assessments performed using this tool would supply useful information to the aerospace community as future standards and guidelines are being developed. Successful regulation will prohibit unsafe operations while clearing the way for operations that do not pose a threat to public safety. Tools such as this risk assessment procedure will help determine what type of operations pose significant risk and which do not so that the policies being developed can reflect the risk associated with various UAS applications in order to maintain a high level of safety.

III. Risk Assessment Framework

Accounting for all possible modes of failure in a given mission is an intractable problem. Therefore this section serves to outline the aspects of UAS risk that are addressed by this model. In essence, this section serves to outline the scope of the proposed model in terms of goals and risk factors which are accounted for in the model.

Risk assessments for UAS operations have the same goal (public safety) as risk assessments for manned aircraft but must take into account the unique flexibility afforded by unmanned aircraft. The risk associated with operating manned aircraft may be divided between three primary groups: the crew and passengers aboard the primary aircraft, the crew and passengers of other nearby aircraft (termed transient aircraft in this paper), and people and property on the ground. When considering the safety of manned aircraft, as long as the first group is always safe, the other two will follow. Manned aircraft must be extremely reliable because any crash or collision is a threat to the people onboard. The area in which the aircraft is operating does not affect the need for reliability.¹⁴

When the crew and passengers are removed from the aircraft, the traditional approach of focusing on the safety of the people onboard the primary aircraft no longer applies. The risk of UAS operations depends not only on the reliability of the aircraft but also on the characteristics of the operating area (air traffic, pedestrians, buildings, etc.). Therefore, the regulations and policies developed for UAS must take both aspects into account if they are to protect the public without unnecessarily inhibiting the development and integration of UAS technologies. For example, policy that allows a 99% reliable UAS to operate over a densely populated area but prohibits a 95% reliable UAS from operating over a remote, unpopulated area would be inadequate. A successful policy must reflect the fact that the true risk is a product of both the aircraft and the operation for which it is used.

The model here will break the risk of UAS operations into three categories: transient aircraft collisions, pedestrian strikes and inhabited building strikes. Collisions within a fleet of UA operating in the same airspace will also be calculated as they could contribute to pedestrian and building strikes. In the absence of established UAS safety standards, the risk assessment results in this project will use the expected number of fatalities per hour as the primary safety metric. In an attempt to give this expectation a more tangible interpretation, an associated insurance risk in terms of dollars per hour is also calculated. Other expectations such as the number of midair collisions and building strikes are also calculated as secondary outputs.

A. Risk Assessment Goals

Risk is a very general term and may be a function of many factors. The formulation of the risk assessment criteria is different depending on the end goal of the assessment. For example, one could attempt to estimate the economic risk associated with a mission. This might include risk due to loss of vehicles or destruction of property in the event of a mishap. Accurately estimating the risk would require information such as the cost to replace lost vehicles, repair the expected damage to other property, and environmental cleanup costs. These costs can be significant, particularly costs to replace vehicles considering that these systems cost on the order of tens of thousands (\$35,000 for an RQ-11 Raven) to tens of millions (\$11M for an MQ-9 Reaper and \$35M for RQ-4 Global Hawk). While an operation which results in a Global Hawk crashing regularly in uninhabited regions may be acceptable from a human safety standpoint, it is clearly not economically viable.

Despite the significant impact of economic risk on business operations of UAS, for the purposes of safely integrating unmanned systems into the NAS, the most important risk assessment is the risk to human safety and loss of life. The model described in this paper is first and foremost concerned with estimating the

potential risk to human safety both aboard other aircraft and on the ground. This model does not take into account the potentially significant economic risk associated with a mission. Furthermore, incorporating these economic costs might obfuscate the human safety aspect, which is the main focus of the project. The dollar amounts attached to human safety risks are not primarily intended to predict the actual cost to insure against human injury (although they may prove useful for this purpose as well) so much as they are intended to be a more tangible representation of the safety risk in the sense that it may be easier to visualize dollars per hour (for insurance) instead of fatalities per hour.

B. Risk Factors

There are numerous ways in which a UAS may fail, and many incidents are the result of multiple factors. In order to improve the reliability of UAS, understanding these specific factors is important so that they may be individually addressed. The causes may be grouped into several categories such as operator error, improper maintenance, loss of communication, equipment failure, weather, etc. Differentiating between types of failures will allow operators and regulators to understand how failure rates might be lowered over time. As a system matures, some causes of failure are largely mitigated (e.g. equipment failure), while other causes tend to persist (e.g. weather). The Air Force Class A Aerospace Mishap records, maintained by the Judge Advocate General's office, are a useful resource for tracking the distribution of mishap causes over time for a particular aircraft system.¹⁵ The Air Force Safety Center offers less detailed mishap data for a number of aircraft, which is useful for finding overall failure rates over time.¹⁶

The Air Force Research Laboratory used these resources in a recent study of Predator mishaps. The study revealed that the first several years of operation were dominated by equipment failures, many of which have been addressed. The system then moved into what the author identifies as a second era dominated by various human factors.¹⁷ Once these causes were better understood, the training for new and current operators was refocused to address the human factors identified as common root causes. Since these changes were implemented, the Predator's Class A mishap rate (per flight hour) has steadily decreased with the greatest improvement being seen in the area of human factors.¹⁸ This study demonstrates how understanding the causal factors of UAS failures can lead to significant improvements in system reliability, which affects both safety and operational costs.

The distribution of mishaps between causal factors is not considered by the risk model developed in this research because it has little effect on the human safety of the current aircraft system. A 'bottom-line' figure for crashes due to all types of failure (including human factors) was deemed sufficient for the purposes of this risk assessment. Those groups wanting to form a risk trajectory to determine when a system will reach a certain level of safety would want to examine the distribution more closely. Understanding the sources of system failures will allow UAS developers and operators to know where critical improvements must be made for a particular platform in order to achieve safety standards. A system level approach² may be of interest for such purposes. An additional reason individual causes of failure were not considered in the risk assessment is to maintain the model's simplicity and ease of use. Every platform will have unique modes of failure and the classification of these failures varies between operators. Accommodating such a high degree of variance would add considerable complexity to the model with little gained in the way of utility.

C. Flight Phases

A further distinction is sometimes made between mishaps based on the phase of flight in which they occur. A typical operation is broken down into taxi, takeoff, climb, enroute, descent, and landing (some operations combine climb with takeoff and descent with landing). Particular activities within the enroute phase, such as loiter, target tracking and target attack may also be specified in cases where they increase the likelihood of a mishap. Studies such as¹⁷ indicate that while the majority of mishaps do occur enroute, a disproportionate number (relative to flight time) occur in other phases. The landing phase, in particular, tends to have a much higher mishap rate relative to the time spent in each phase.

The model considered here does not distinguish between mishaps in different phases of flight, which makes the implicit assumption that the failure rate being used excludes mishaps during particular flight phases that do not fit the general population profile (e.g. isolated airfields, restricted areas). For the purposes of public safety, neglecting the phases of flight that do not have a realistic possibility encountering humans or other aircraft is justifiable.

The taxi, takeoff and landing phases often take place through predefined paths over airports or airfields that are free of homes and pedestrians. If a particular UAS is prone to crash during takeoff, for example, the operator may choose to always perform takeoff in a restricted area free of pedestrians and populated buildings. This would mitigate the safety risks of mishaps during takeoff, meaning they should not be included in the overall failure rate since the area in which takeoff occurs does not fit the population profile of the general operating area.

Bird strikes, on the other hand, are a far greater risk during taxi, takeoff and landing, with 80% occurring below 1,000ft AGL and 96% occurring below 5,000ft AGL.¹⁹ A risk assessment focusing on the total economic risk would need to consider mishaps during all phases of flight. While crashing UA on the runway is not a threat to public safety, doing so will result in expensive repairs and aircraft downtime. The failure rate for each phase would need to be specified individually since mishaps during different phases of flight will tend toward different causes and are likely to result in different costs. The repair/replacement costs are expected to be higher for enroute failures (which will likely destroy the UA) while takeoff and landing incidents often only require repair. The lack of pedestrians and populated buildings beneath takeoff and landing paths results in much less risk of causing a fatality or property damage during these flight phases.

IV. Risk Model

As stated previously, the two potential causes for injury to humans are midair collisions, which affect persons aboard transient aircraft, and ground collisions, which affect pedestrians and those located inside buildings.

A. Midair Collisions

The midair collision calculations used here are based on theory originally developed to predict the collision frequency of gas molecules.²⁰ This theory¹ was similarly applied to air traffic in prior literature^{21,22}. The collision frequency between a single UA and transient air traffic is a product of the transient aircraft density, the combined frontal areas and the velocity of both the UA and the transient aircraft.

We define ρ_o to be the density of transient aircraft per km³, ϕ_o and ϕ_{ua} to be the frontal area in km² of the transient aircraft and the UA, V_o and V_{ua} as the velocity in km/hr of the transient aircraft and the UA.

The following analysis is performed from the perspective of a single UA. To average the risk of a midair collision over all orientations, the frontal areas of the UA and the transient aircraft are recast as circles of radii $R_{ua} = \sqrt{\phi_{ua}/\pi}$ (km) and $R_o = \sqrt{\phi_o/\pi}$ (km). A collision will occur if the centers of the aircraft are within a distance $R_{ua} + R_o$. The instantaneous collision area is therefore

$$\phi_{col} = \pi(R_{ua} + R_o)^2 = \phi_{ua} + \phi_o + 2\sqrt{\phi_{ua}\phi_o} \quad (1)$$

Assuming that the transient aircraft are stationary ($V_o = 0$), the volume of collision airspace that the UA sweeps out in a time ΔT is simply $V_{col} = \phi_{col}V_{ua}\Delta T$. The number of collisions is a product of the collision volume and the transient aircraft density. Dividing by the time ΔT gives the expected collision rate for a single UA with stationary transient aircraft.

$$\hat{F}_{transient} = \rho_o\phi_{col}V_{ua} \quad (2)$$

To correct for the fact that the transient aircraft are not stationary ($V_o \neq 0$), V_{ua} is replaced with a relative velocity. Previous literature²⁰ suggests an additive term such as $V_{rel} = \sqrt{V_{ua}^2 + V_o^2}$. However, to develop a conservative model of collisions, it is assumed that all transient aircraft are flying opposite of the UA (to create the largest possible collision volume).

$$V_{rel} = V_{ua} + V_o \quad (3)$$

Assuming that UA collisions are independent of each other, the total collision rate for the fleet of UA is simply obtained by multiplying Eq. 2 by the number of UA in the fleet and replacing V_{ua} with V_{rel} .

$$\tilde{F}_{transient} = N_{ua}\rho_o\phi_{col}V_{rel} \quad (4)$$

To make the calculation more accurate in a wide range of operations, collision avoidance capabilities must be incorporated. Any UAS that are allowed to fly in non-restricted airspace will likely be required to be

equipped with a transponder (such as the Microair T2000UAV-L) making them visible to air traffic control (ATC) and Traffic Collision Avoidance System (TCAS) equipped aircraft. Having a transponder will greatly reduce the risk of midair collisions between UA and TCAS equipped aircraft. In addition to a transponder (which broadcasts its own location but does not “see” nearby aircraft itself), UAS will eventually incorporate active SAA systems. These systems will enable the UAS to actively avoid collisions with transient aircraft and other UA whether or not they are cooperative.

Collision avoidance gained from the airspace structure or procedural separation will have to be incorporated into the UA collision avoidance and transient aircraft collision avoidance terms. The basic collision model assumes all aircraft fly randomly within the specified volume with no structural or procedural separation.

These collision avoidance procedures are incorporated into the midair collision model as mitigating probabilities. We define ϵ_o as the probability that a given transient aircraft will avoid a collision with another transient AC or UA when a collision would be imminent if no avoidance actions are taken. This is therefore a scalar value in the range 0 to 1 with 0 implying that the aircraft is essentially flying blind and will never maneuver to avoid a potential collision and 1 implying that the transient aircraft has perfect collision avoidance and will avoid all potential collisions. In a somewhat similar fashion, we define $\epsilon_{ua/o}$ as the collision avoidance of a given UAS with transient AC and $\epsilon_{ua/ua}$ as the collision avoidance of a given UAS with other UAS within its own fleet. The term $\epsilon_{ua/o}$ can be thought of as the cumulative efforts of whatever SAA algorithm is aboard the UA. Typically, most UAS have collision avoidance algorithms with respect to other agents in its own fleet, so $\epsilon_{ua/ua}$ measures the effectiveness of this algorithm. Given that most UAS have explicit knowledge of the locations of other agents within its own fleet, $\epsilon_{ua/ua}$ is typically greater than $\epsilon_{ua/o}$.

In the situation of a potential collision between a UA and a transient AC, the transient AC will fail to avoid a collision $1 - \epsilon_o$ percent of the time and similarly, the UA will fail to avoid the collision $1 - \epsilon_{ua/o}$ percent of the time. In order for a collision to occur, both the transient AC and the UA collision avoidance systems must fail simultaneously. Assuming that these events are independent, the expected collision rate of the UA fleet and transient AC with collision avoidance taken into account is given by

$$F_{transient} = N_{ua}\rho_o\phi_{col}V_{rel}(1 - \epsilon_{ua/o})(1 - \epsilon_o) \quad (5)$$

To verify the model in Eq. 5, a 3 dimensional Monte Carlo simulation is run using a range of V_o and V_{ua} values. A picture of the environment at a given instance in time is shown in Figure 1(a). This simulation is used to generate a series of “experimental” data which can be used for several purposes. First, this can be used to validate the models of midair collision rates such as in Eq. 5. Secondly, it can be used as input to various learning algorithms²³ to attempt to learn different models which describe the underlying physics of the situation. One such learning algorithm proposes that the models $V_{rel} = \max(V_o, V_{ua})$ fits the given data well. One benefit of this risk framework is that it is modular in the sense that the assessor can choose different models for different components and easily view the ramifications of this choice. For example, the various models for V_{rel} described previously are shown in Figure 1(b).

As can be seen from Figure 1(b), the model of $V_{rel} = \sqrt{V_o^2 + V_{ua}^2}$ fits the data quite well for most scenarios. Note that at low velocities, it tends to underestimate $F_{transient}$. Similarly, the model from the learning algorithm also appears to underestimate the crash rate for almost all conditions. In the context of risk assessment, it is better to err on the side of caution and overestimate the failure rate rather than underestimate it. As can be seen, the proposed model of Eq. 3 is a fairly simple, justifiable model that provides a conservative estimate of $F_{transient}$ for all conditions. It should be noted that the fits provided by all proposed models fall well within an order of magnitude of the simulated results.

Note that $F_{transient}$ is the collision rate between the UA fleet and transient AC. A similar analysis can be performed to estimate collision rates between UA within their own fleet. This involves using the previous equations with substitutions of $V_o = V_{ua}$, $\phi_o = \phi_{ua}$, and $\rho_o = \rho_{ua}$.

$$\rho_{ua} = (N_{ua} - 1)/\eta_{fleet} \quad (6)$$

The term ρ_{ua} is the density of UA. Previously, the density of transient aircraft was assumed to be uniformly spread over the operating volume. With in-fleet UA operations, there may be missions where the UA may be spread out uniformly over the operating area. These might include search and rescue,²⁴ environmental surveying,²⁵ or area patrol.²⁶ In these situations, $\eta_{ua} \approx \eta_{ops}$. However, there are other missions²⁷ where the fleet of UAS are in close proximity to each other or otherwise spaced such that a

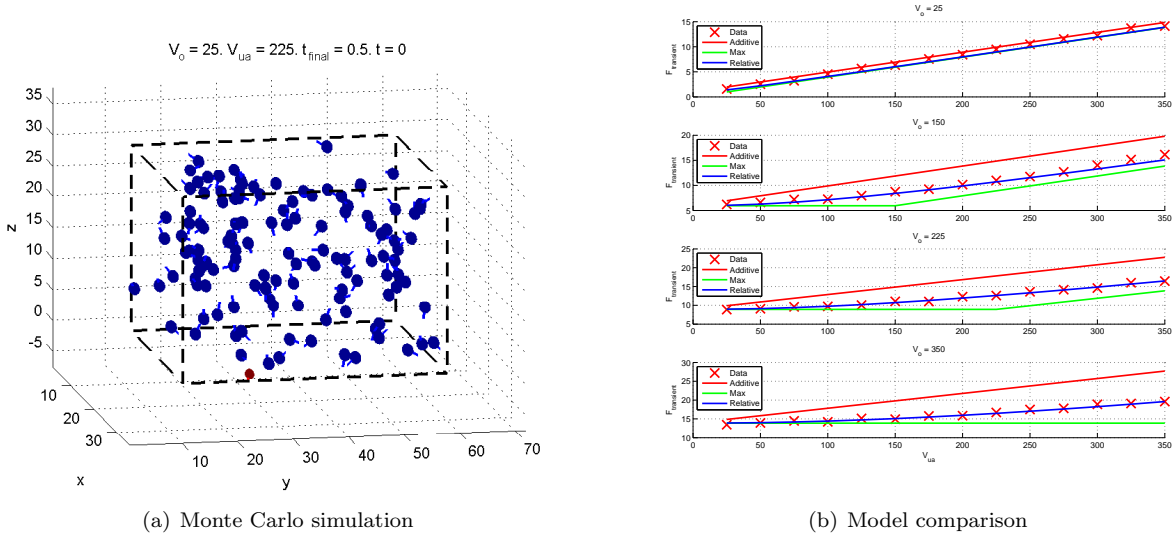


Figure 1. $F_{transient}$ for various cases of V_o and V_{ua} . Additive model uses $V_{rel} = V_o + V_{ua}$ (Eq. 3), max model uses model learned by Eureka of $V_{rel} = \max(V_o, V_{ua})$, and relative model uses $V_{rel} = \sqrt{V_o^2 + V_{rel}^2}$. All scenarios use $\rho_o = 0.004$, $\phi_o = 3$, $\phi_{ua} = 2$, $\epsilon_{ua/o} = \epsilon_o = 0$.

uniform density over the entire operating volume is not a reasonable assumption. In this situation η_{fleet} may be small compared to η_{ops} .

Once the mission has been selected, the appropriate volumes can simply be calculated using $\eta_{ops} = A_{ops}(z_{max} - z_{min})$ and $\eta_{fleet} = A_{ops,fleet}(z_{max,fleet} - z_{min,fleet})$.

The expected in fleet collision rate is therefore

$$F_{fleet} = N_{ua}\rho_{ua}(4\phi_{ua})(V_{rel})(1 - \epsilon_{ua/ua})^2 \quad (7)$$

Once again, in Eq. 7, the term V_{rel} can be computed using Eq. 3 where $V_{rel} = 2V_{ua}$ for a more conservative estimate or using $V_{rel} = \sqrt{2}V_{ua}$ for a more accurate estimate.

Note that both Eq. 5 and Eq. 7 estimate the rate of collisions between a UA and another aircraft (either a transient aircraft or another UA, respectively). Each collision actually produces two affected aircraft. For example, if $F_{transient} = 6$, then it can be expected that 6 UA will collide with 6 transient aircraft per flight hour for a total of 12 affected aircraft which will eventually crash and strike the ground. In a similar fashion, if $F_{fleet} = 2$, then it is expected that 2 UA will collide with another 2 UA per flight hour for a total of 4 affected UA.

The total number of midair collisions, α , (both between UA and transient aircraft and between UA and other UA) during a mission is simply the sum of $F_{transient}$ and F_{fleet} multiplied by the mission length, M_L . Note that M_L is the length of the mission, not the aircraft-hours. For example, if 3 UA fly a mission for 5 hours, then $M_L = 5$. The difference between collision rate and crash rate is further explained later in Eq. 13.

$$\alpha = M_L(F_{transient} + F_{fleet}) \quad (8)$$

B. Ground Collisions

The ground collision calculations (pedestrians and buildings) are a hybrid of the equations²¹ developed in prior²² literature²⁸ to best represent general UAS operations. The risk to people and buildings from crashes due to system failures (i.e. not from midair collisions) is found by assuming that upon failure, the UA glides to the ground at maximum L/D (worst-case scenario) with glide angle γ . The associated geometry is shown in Figure 2.

The risk to people on the ground from midair collisions assumes upon midair collision, the UA will approach the surface in vertical free fall. The expected number of building and pedestrian strikes is composed

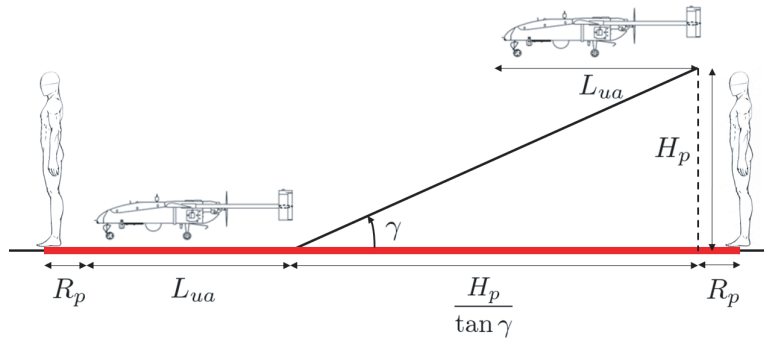


Figure 2. Geometry showing affected distance covered by UA during a horizontal, gliding crash (red distance). The total affected area is this distance multiplied by the wingspan of the UA plus $2R_p$.

of two calculations that take each case (glide and free fall) into account. For example, if the UA has a system failure and glides horizontally to the ground, the danger areas to pedestrians and buildings are given by

$$A_{L_{H_p}} = (w_{ua} + 2R_p)(L_{ua} + \frac{H_p}{\tan \gamma} + 2R_p) \quad (9)$$

$$A_{L_{H_b}} = (w_{ua} + w_b)(L_{ua} + \frac{H_b}{\tan \gamma} + w_b) \quad (10)$$

In a similar fashion, if the UA sustains midair collision, it is assumed that it will fall vertically to the ground. In this case the affected areas for pedestrians and buildings become

$$A_{L_{V_p}} = \pi(\frac{\max(w_{ua}, L_{ua})}{2} + R_p)^2 \quad (11)$$

$$A_{L_{V_b}} = \pi(\frac{\max(w_{ua}, L_{ua})}{2} + \frac{w_b}{2})^2 \quad (12)$$

In Eq. 9-12, A_{L_H} and A_{L_V} are the lethal areas in km^2 for aircraft gliding horizontally and falling vertically, A_b is the average building size in km^2 , w_b is the average building width in km (defined as $w_b = \sqrt{A_b}$), H_b is the average building height in km, R_p is the radius of a person (defined as 2.5E-4km or 0.25m), H_p is the height of a person (for a standing pedestrian, defined as 1.75E-3km or 1.75m), γ is the UA glide angle without power, w_{ua} is the UA wingspan in km, and L_{ua} is the UA length in km.

The number of aircraft crashes are a function of both $F_{transient}$ and F_{fleet} . Recall Section IV.A describes how a single collision affects 2 aircraft. The rate of aircraft crashes (ground strikes) per hour is therefore

$$C_{midair} = 2(F_{transient} + F_{fleet}) \quad (13)$$

Note that this model does not differentiate between the types of aircraft crashes. Eq. 13 and Eq. 9-12 assume that the crashing aircraft has the dimensions of the UA. A more complex and perhaps slightly more accurate model would differentiate between a crash of a UA and a crash of a transient AC. This would involve two parallel computations, one to record crash rate and danger areas for crashed transient AC ($C_{midair,o} = F_{transient}$) and another to record crash rate and danger areas for crashed UA ($C_{midair,ua} = F_{transient} + 2F_{fleet}$). The obvious drawback to this approach is then requiring information regarding dimensions of the transient AC in question.

The number of pedestrian and building strikes per hour is then a combination of system failures and midair collisions.

$$F_{ped} = F_{ped,p} + F_{ped,midair} \quad (14)$$

$$F_{bldg} = F_{bldg,p} + F_{bldg,midair} \quad (15)$$

$$\begin{aligned}
\text{where } F_{ped,p} &= N_{ua}\lambda\sigma_p A_{LHp} \\
F_{ped,midair} &= C_{midair}\sigma_p A_{LVp} \\
F_{bldg,p} &= N_{ua}\lambda\sigma_b A_{LHb} \\
F_{bldg,midair} &= C_{midair}\sigma_b A_{LVb}
\end{aligned}$$

In these expressions, λ is the UAS midair failure rate per hour from all sources for a single UA. This is typically cited by manufacturers as the mean time between failure for a single aircraft. σ_b and σ_p are the building and pedestrian densities (respectively) per km². Separating the strike rate due to system failures and midair collisions will prove insightful in later analysis.

Since UAS tend to have high mishap rates during takeoff and landing, the failure rate used will only represent mid-flight failures if takeoff and landing are performed in a restricted area free of pedestrians. This distinction is made in order to avoid overestimating the risk. If takeoff and landing do not take place in a restricted area, then these mishaps should be included in the failure rate (see Section III.C).

C. Fatalities and Insurance

A successful risk assessment must communicate the results in a way that provides the user with a tangible sense for the risk involved. The most *important* result is the number of fatalities expected. Unfortunately, hearing a number like 2.3E-7 fatalities per hour will not mean much to most users. Though doing so may sound insensitive, a simple way to make this number more tangible is to look at the cost to insure the operation. An amount of liability coverage is chosen per fatality, which results in a cost to insure the operation per hour. Many other factors could be considered in the liability coverage such as property damage, damage to transient aircraft, damage to the UA themselves, etc. However, the fatality liability will be the dominate cost and also the best indicator of the most important risks involved.

The expected number of fatalities per hour is given by

$$F_{fat} = F_{fat,p} + F_{fat,midair} \quad (16)$$

$$\begin{aligned}
\text{where } F_{fat,p} &= F_{ped,p}D_{ped} + F_{bldg,p}D_{bldg} \\
F_{fat,midair} &= F_{ped,midair}D_{ped} + F_{bldg,midair}D_{bldg} + F_{transient}P_o
\end{aligned}$$

In Eq. 16, D_{ped} is the fatality rate for a pedestrian strike. It is defined as the average number of fatalities incurred when a UA strikes a pedestrian and is therefore in range of [0, 1]. Currently this is an independent parameter for the risk assessment but other work²⁹ has investigated the kinetic energy associated with the UA and its correlation to a lethal strike. Future improvements would estimate this parameter automatically based on UA velocity and weight. Other work has suggested that any UA above 2 lb is capable of causing life threatening injuries² (corresponding to $D_{ped} = 1$). D_{bldg} is the fatality rate for a building strike (in range of [0, all people in building]). This allows versatility in modeling hard structures where people are more protected vs. softer structures such as residential homes. P_o is the average number of passengers on a transient aircraft. The model assumes that a collision between a UA and a transient AC causes the death of all passengers aboard the transient AC.

Once again, the expression for F_{fat} is broken up into fatalities caused by midair collisions ($F_{fat,midair}$) and fatalities caused by system failures ($F_{fat,p}$).

The cost to insure the operations per hour is a product of the I_{fat} , the insurance liability per fatality, and the expected fatality rate

$$M = F_{fat}I_{fat} \quad (17)$$

The total cost to insure the mission is therefore $M * M_L$.

V. Results and Validation

The model presented in Section IV presents a conservative estimate of collisions, crashes, and fatalities for UAS operations. This model can now be validated using historical data and other methods.

A. Midair Collision Validation

Random collision theory has been shown to be a valid model for estimating aircraft collisions for VFR (visual flight rules) traffic.¹ These works aimed to measure the degree to which human efforts at collision avoidance were effective. To show that the midair collision model presented in Section IV.A is a reliable method of estimation, results predicted by the model will be compared with historical data. Historical data of total aircraft flight hours, H , and total midair collisions, α_H , is available as inputs.¹ To model historical midair collisions, we use consider the population of general aviation aircraft as a large fleet of UA and apply Eq. 7. Parameters of Eq. 7 can be computed from the historical data as follows. Assuming that on average, aircraft fly around the clock, then $M_L = 365 \times 24 = 8760$ hours. This accounts somewhat for the heavier traffic during daylight hours and lighter traffic at night. Using this information, the average number of vehicles in the air at any given time can be calculated as $N_{ua} = H/M_L$. The volume of the mission area, η_{fleet} is assumed to be the entire United States ($9,182,316 \text{ km}^2$) with aircraft distributed uniformly from sea level to 3.04 km ($10,000 \text{ ft}$). The density of UA, ρ_{ua} , is then computed using Eq 6. The cross sectional area of the representative UA is computed by first obtaining the cross sectional area of a Kitfox Classic IV which is a small, single engine, two seater aircraft which is typical of a smaller general aviation aircraft from the time period in question. This is shown in Figure 3.

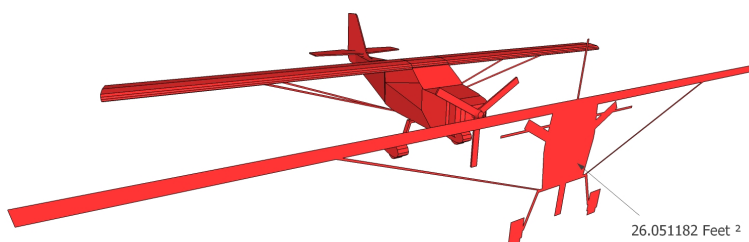


Figure 3. 3D and cross sectional area calculation of a Kitfox Classic IV which is typical of a small, general aviation aircraft. Cross sectional area is $26.05 \text{ ft}^2 = 2.42 \times 10^{-6} \text{ km}^2$. Cruise velocity is $85 \text{ mi/hr} = 136.8 \text{ km/hr}$.

To account for the fact that most other aircraft in this time period were this size or larger (turboprops, jets, rotorcraft, gliders, etc.), the cross sectional area used is $\phi_{ua} = 2 * (2.42 \times 10^{-6}) \text{ km}^2$. In a similar fashion, we assume that $V_{ua} = 2 * (136.8) \text{ km/hr}$.

At this point, all the parameters for Eq. 7 are accounted for and the predicted number of collisions is simply $\alpha = M_L F_{fleet}$ (assuming no collision avoidance). These results are presented in Table 1.

Table 1. Predicted and actual midair collisions for time period between 1969 and 1978. Parameters used for model are $M_L = 365 \times 24 \text{ hr}$, $\phi_{ua} = 2 * (2.42 \times 10^{-6}) \text{ km}^2$, $V_{ua} = 2 * (136.8) \text{ km/hr}$, and $\eta_{fleet} = 9,182,316 \times 3.04 \text{ km}^3$.

Year	Flight Hours H	Actual Collisions α_H	Predicted Collisions α	Collision Avoidance $\epsilon_{ua/ua}$
1969	25351000	23	27.83	0.0910
1970	26030000	32	29.34	-0.0442
1971	25512000	27	28.19	0.0213
1972	26974000	24	31.51	0.1273
1973	29974000	24	38.91	0.2147
1974	31413000	32	42.74	0.1347
1975	32024000	28	44.42	0.2061
1976	33922000	30	49.84	0.2242
1977	35792000	34	55.59	0.2172
1978	36600000	33	58.02	0.2459
Average	30359200	28.7	40.63	0.1438

In Table 1, we see that the model presented in Eq. 7 is fairly accurate and provides a good order of magnitude approximation. Given the many assumptions made to arrive at this result, the accuracy and ability of the model to predict actual midair collisions is surprising. As expected, the model is slightly conservative and seems to consistently over predict the number of collisions. This is possibly because the results for α do not take into account mitigating factors such as active collision avoidance. The effective collision avoidance required so that $\alpha = \alpha_H$ is shown in the last column as $\epsilon_{ua/ua}$. Averaged over all years yields $\epsilon_{ua/ua} = 0.1438$, showing that for the most part, random gas molecule collision is a fairly representative model of actual midair collisions. According to this model and historical data, in situations where a midair collision was imminent, pilots only successfully avoided a collision 14.38 percent of the time.

A similar analysis can be done for a more recent data set between the years of 1995-2005. The model of the aircraft is updated to account for larger, faster aircraft with a higher service ceiling in this time period. The results and associated parameters are shown in Table 2.

Table 2. Predicted and actual midair collisions for time period between 1995 and 2005. Parameters used for model are $M_L = 365 \times 24$ hr, $\phi_{ua} = 4 * (2.42 \times 10^{-6})$ km², $V_{ua} = 350$ km/hr, and $\eta_{fleet} = 9,182,316 \times 5$ km³.

Year	Flight Hours H	Actual Collisions α_H	Predicted Collisions α	Collision Avoidance $\epsilon_{ua/ua}$
1995	24000000	29	38.80	0.1355
1996	24900000	35	41.77	0.0846
1997	25500000	28	43.81	0.2005
1998	25500000	37	43.81	0.2149
1999	29700000	31	59.43	0.2778
2000	29100000	25	57.05	0.3380
2001	25400000	12	43.47	0.4746
2002	25500000	10	43.81	0.5222
2003	25900000	20	45.19	0.3348
2004	24800000	22	41.44	0.2713
2005	23100000	20	35.95	0.2541
Average	25763636	23.55	44.96	0.2826

Once again, the random gas collision model without collision avoidance predicts a similar number of collisions. The average collision avoidance appears to have increased to the point where pilots are avoiding imminent collisions approximately 28 percent of the time thereby suggesting that sense-and-avoid and see-and-avoid technologies are becoming more effective, but not by much.

The fact that midair collisions did in fact occur (just 30 years ago) at a rate very close to that predicted by random collision theory demonstrates the applicability of the theory. Although the current data shows some improvement over that of the 1970s, random collision theory still provides an order-of-magnitude approximation. When information about the aircraft's collision avoidance (established experimentally) can be incorporated, the prediction will become more accurate.

Midair collisions involving air carriers, which operate under instrument flight rules (IFR), are far less frequent and show human efforts to avoid midair collisions have been highly effective. For this reason, the midair collision model of Section IV.A does not accurately approximate the collision rate for IFR traffic. Several reasons exist for the significant difference in how effective human efforts have been between the two categories. Virtually all air carriers (≥ 10 seats) are required to be equipped with TCAS which uses transponder signals to notify the pilot of potential collisions or "intruder aircraft". Additionally, air carriers spend the vast majority of their time in Class A airspace which requires the aircraft to be under ATC control and operating under IFR. Finally, most air carrier flights follow simple point-to-point flight paths at set altitudes. All of these characteristics are in contrast to general aviation flights which are not always equipped with transponders and typically operate in Class E airspace which does not require ATC communication or IFR. Not surprisingly, air carriers avoid midair collisions far better because far more technological and systematic collision avoidance is in place for air carrier operations.

General aviation provides a better baseline for comparison to *near-term* UAS operations than air carriers.

Until the ADS-B equipped NextGen ATS is implemented and much more effective SAA technology has been developed, UAS are not likely to achieve anywhere near the avoidance capability of air carriers. UAS are also likely to have variable flight paths that may wander and change altitudes depending on the application, much more similar to general aviation than air carriers. More importantly, the niche operations that UAS are likely to fill can accept less reliable avoidance and still present risk-levels equivalent to or less than the risk-levels of current manned aircraft operations. Air carrier-like avoidance is not necessary for all applications in order to protect human safety.

VI. Example Calculations

This section presents sample calculations for three scenarios. The first two scenarios are operations which show a potentially viable operation for UAS and the third illustrates an operation which does not appear to be a good fit for UAS. Note that all calculation results are presented to several significant figures for the purpose of allowing the reader to reproduce results. The results are should only be considered accurate to an order of magnitude due to the significant error associated with some of the input parameters.

A. Scenario 1: Border Patrol

In recent years a number of technologies have been adapted by the United States Customs and Border Protection (CBP) Agency to help protect and monitor U.S. coastlines and borders, including UAS as one of the key technologies to augment the agency’s border patrol capabilities. Several General Atomics MQ-9 Reapers, for instance, are being operated over the Arizona-Mexico border to spot smugglers and people entering the country illegally.³⁰ According to recent reports, the government is planning to expand the use of UAS to other border regions as well,

“Customs and Border Protection has said it intends to increase unmanned aircraft systems across the country this year, and it expects a complete network of the unmanned planes all along the border by 2015.

Officials boasted about the Predators’ effectiveness in a fact sheet published in February 2009. They reported that Predator B planes have flown more than 1,500 hours and contributed to the seizure of more than 15,000 pounds of marijuana and the apprehension of more than 4,000 undocumented people.”³¹

1. UAS Properties

The wingspan, length and operating speed of the MQ-9 Reaper are readily available as 20m, 11m and 162kts.³² By referencing pictures and diagrams of the Reaper, see Figure 4, we can estimate the frontal area with the landing gear up. We start by drawing a triangle encompassing the propeller and tail assembly. The width across the top of the triangle is 6.8m and the height from top to bottom of the tail is 3m, giving an area of $\approx 10 \text{ m}^2$. The wings will be approximated as two rectangles 0.5m high and 8.5m wide (20m wingspan minus $\approx 3\text{m}$ overlapped by the tail section). The total frontal area is then approximately 18.5m^2 . The frontal area approximation is depicted in Figure 5.

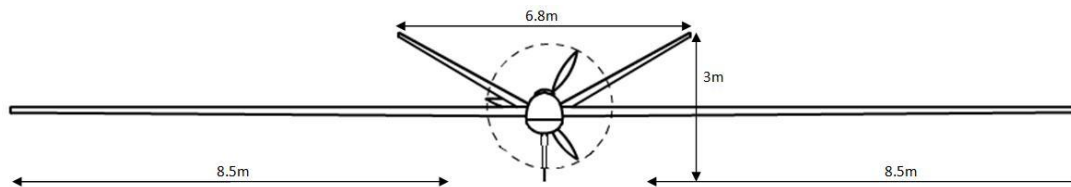


Figure 4. MQ-9 Reaper frontal area dimensions.

The lift to drag ratio is not published, but this information would certainly be available to a group operating the Reaper. We can safely approximate the lift to drag ratio at about 25:1 which yields a glide angle of $\tan^{-1}(1/25) = 2.3^\circ$. Based on the Reaper’s flight history, it has an established Class A mishap

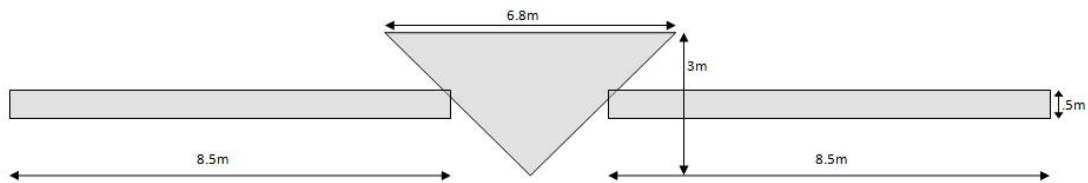


Figure 5. MQ-9 Reaper frontal area approximation.

(\$1M+ damage or fatality) rate of 15.3 per 100,000 flight hours (1.53E-4 crashes/ft hr).³³ The UAS control center is certain to know the location of all Reapers in the air, and every Reaper is operated by its own pilot, so in-flight collision avoidance should be very reliable. To allow for the possibility of a communication loss, an in-flight collision avoidance of 90% will be used.

Reapers are equipped with Mode C transponders, which will aid other aircraft in avoiding collisions with the Reaper, but this fact does not mean that the Reaper will be able to sense other aircraft. The UAS pilots can monitor air traffic using ground-based radar, but since UAS are not designed to perform aggressive maneuvers and occasionally suffer communication losses, we will assign the UAS a collision avoidance of only 0.7 (70% effective). This figure is an estimate for the purposes of this example. In a real risk assessment, the operator must determine the collision avoidance term based on experimental or historical data.

2. Operating Area

The CBP operates four MQ-9 Reapers along the 600km Arizona-Mexico border. We will assume they patrol the territory within 20km of the border (distance between the border and the UAS base in Sierra Vista) which gives a 12,000 km² operating area. A typical operating altitude for the Reaper during this type of observation is 5.5-7.5km (FL180-FL246). The Reaper can operate at much higher altitudes, but we are only interested in the range being used for this particular operation. Since details on the CBP's use of the Reapers are not published, we will consider the case where three of the four Reapers are in the air at any given time around the clock.

To determine the population density, we will use the data available from the U.S. Census Bureau, refined by the information we can gather from Google Maps satellite images. Looking at the 5-digit zip-code population data for the area along the border will give us a baseline population density. The population and home densities for the zip codes along the border are shown in Table 3. The average population density is 4.6 people/km² and the average housing unit density is 1.9 homes/km². If the zip codes for the three biggest cities on the border (Douglas/Agua Prieta, Nogales & Yuma/San Luis) are excluded we lose only 7% of the land area while avoiding 48% of the population. This assumption leaves a population density of 2.6 people/km² and 1.4 homes/km².

Assuming the Reapers do not operate over the three aforementioned cities (other than takeoff and landing near Nogales) is justifiable because they focus on illegal border crossings in more remote stretches, away from checkpoints and land-based law enforcement. Focusing the operation in these more remote areas minimizes the risk to the public and allows the UAS to complement the CBP at their weakest points. The home density can be used for the overall building density if we assume everyone in the population is either an exposed pedestrian or in their home at any given time. Considering most people spend the majority of their time indoors (school, work, home), we will take 10% of the population (0.26 people/km²) to be exposed pedestrians and the remaining 90% to be indoors. The average housing unit then has 1.7 people inside at any given time.

Since the Reaper is a heavy, sturdy aircraft that moves at high speeds, the pedestrian strike fatality rate will be taken as 1 (i.e. 100%). The building structure offers some protection to people indoors, but the size/weight/speed combination of the Reaper still poses a threat. Since all buildings are being modeled as homes we will estimate that a strike will result in the death of 25% of the people inside which gives a fatality rate of 0.42 deaths/strike. The average home can be taken as having a 200 m² footprint and being 5m high.

Table 3. Population data for Arizona ZIP codes on the border.

Zip Code	Area (km^2)	People/ km^2	Population	Homes/ km^2	Homes
85608	1275.2	0.1	98	0.0	49
85607	947.9	22.3	21117	7.4	6990
85603	703.0	12.2	8577	6.3	4424
85615	590.6	11.1	6544	4.7	2805
85624	972.6	1.4	1314	0.8	789
85621	629.8	36.3	22881	11.5	7246
85634	7477.9	0.8	6063	0.3	2021
85633	870.7	0.2	134	0.1	67
85321	6133.8	0.8	4973	0.5	3079
85365	6737.8	5.4	36161	3.1	20812
85350	270.8	53.7	14556	12.5	3378
Totals	26610	4.6	122420	1.9	51660

3. Transient Aircraft

To estimate the air traffic in the region, we will use Flight Explorer Personal Edition and consult regional aeronautical charts. The altitude range under consideration is in Class A airspace so any air traffic through the region will be equipped with a transponder and most should be visible to the Flight Explorer tracking system (though some military flights, for instance, may not show up). Monitoring the airspace over Southern Arizona reveals that very little air traffic exists near the border. Figure 6 shows typical traffic for Southern Arizona. Most of the air traffic that is present passes over Nogales or Yuma which have already been excluded from our operating area. Aeronautical charts of the region show the only jetway (high altitude airway) that crosses the Arizona border, J92, originates at Tucson International and passes over the border at Nogales, not in our operating space.

A large portion of the airspace is sectioned off as restricted or military operation areas (MOAs). This restriction certainly influences the meager air traffic at low altitudes but most restricted areas and MOAs do not extend above FL180 into Class A airspace so the lack of high altitude air traffic is mostly natural. Monitoring the air traffic for several hours a day over three days (a larger sampling would be needed for a ‘real’ risk assessment), only two aircraft briefly passed over the region of interest but were not in the altitude range of interest. Based on this sampling, we can conservatively estimate that the probability of an aircraft being in the region of interest is no more than 10% which gives an expected air traffic density of $0.1/12,000 \approx 8 \times 10^{-6}$ aircraft/ km^3 .

Given the altitude range, the air traffic will be divided close to evenly between the commercial jet and regional jet classes. The risk calculator’s predefined models will be used for both classes. As discussed previously, all air traffic in Class A airspace will be under ATC control operating under IFR and equipped with effective collision avoidance systems and practices. A conservative collision avoidance of 0.95 (95% effective) will be assigned to each transient aircraft model.

A liability of \$10,000,000 per fatality is assumed. All of the parameters relevant to this calculation are summarized in Table 4.

Table 4: Border patrol parameters.

Parameter	Value	Comment
UAS		
V_{ua}	162 knots	-
ϕ_{ua}	18.5 m^2	-
w_{ua}	20 m	-

continued on next page...

Table 4 – Continued

Parameter	Value	Comment
L_{ua}	11 m	-
γ	2.3 degrees	from estimated L/D ratio
λ	15.3/100000	from historical class A mishap rate
$\epsilon_{ua/o}$	0.5	-
$\epsilon_{ua/ua}$	0.9	-
$z_{max,fleet}$	7.5 km	-
$z_{min,fleet}$	5.5 km	-
$A_{ops,fleet}$	12000 km ²	team distributed over region
Op Area 1		
N_{ua}	3	-
z_{max}	7.5 km	-
z_{min}	5.5 km	-
M_L	8760 hours	1 year operation
A_{ops}	12000 km ²	-
σ_b	1.4 buildings/km ²	-
A_b	200 m ²	-
H_b	5 m	-
D_{bldg}	0.42 fatalities/strike	-
σ_p	0.26 people/km ²	excluding populated areas
H_p	1.75 m	-
R_p	0.25 m	-
D_{ped}	1 fatalities/strike	100% mortality rate
Transient AC 1		
Applied Op Area	1	-
ρ_o	4.167×10^{-6} AC/km ³	-
V_o	432 knots	-
ϕ_o	80 m ²	-
P_o	45 people/AC	regional jets
ϵ_o	0.95	AC under ATC
Insurance		
I_{fat}	10,000,000 dollars/fatality	-

4. Risk Assessment Results

Using these parameters, the model outputs values as shown in Table 5. The first two columns are the values as described in Section IV. Recall that these are defined as a per hour rate of occurrence. Because the mission persists for M_L hours, the number of occurrences during the mission can be obtained by multiplying by M_L . This can also be thought of as an occurrence rate per mission. The resulting per mission rate can then be inverted to obtain the number of missions between occurrences. In this situation, since the mission persists for 1 year, this can also be thought of as the number of years between incidents. This value is shown in the third column.

The interesting result is the order of magnitude difference in fatalities due to midair collisions (1 every 420 years) and general system failures (1 every 75 years). Although the operation expects 1 fatality every 64 years, the cause of this fatality is most likely due to a general system failure rather than a midair (either transient or in fleet) collision. Tracing the cause further back, in the already unlikely situation of a midair collision causing a fatality, this midair collision is almost certainly an in-fleet collision instead of collision

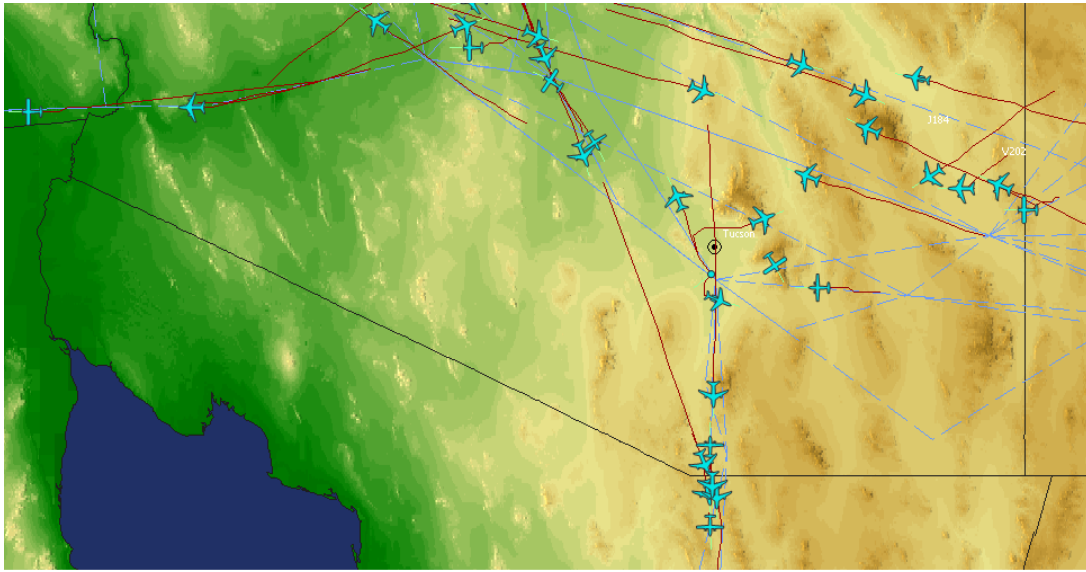


Figure 6. Airspace over Southern Arizona (from Flight Explorer PE).

with a transient aircraft (F_{fleet} is more than 18 times higher than $F_{transient}$) despite the fact that in-fleet collision avoidance is significantly better than transient aircraft avoidance. This stems from the fact the density of UA is 200 times more than transient aircraft in this operating area.

These results suggest that more lives can be saved by spending more time and effort into making UAS systems more robust and less susceptible to general system failures rather than spending excessive time on sense and avoid technologies to avoid transient collisions. Further improvements to in-fleet collision avoidance would also lower the fatality rate. These are beneficial results because these types of technology would be implemented by the UAS manufacturer and would only involve internal improvements and developments on the system itself rather than trying to account for external sources (ie transient aircraft).

If every fatality is covered by a \$10 million insurance policy, the price to insure the operation is roughly \$17.85 per hour, which gives an annual cost of about \$156,375 for the team of Reapers. This cost is intended to be a more tangible expression of human safety risk rather than an estimation of what any actual insurance policy would cost.

These risk-associated costs are undoubtedly quite small compared to the overall costs of operation since the Reaper itself costs \$10-20 million each (depending on what is included). The hourly insurance risk is in fact much less than the cost of paying UAS pilots and crew to operate the Reaper. This result does not mean that the operation is completely safe, but rather it indicates a, presumably, acceptable risk-level for this operation. Note that manned aircraft with the same reliability present far too much risk, regardless of where they are operated, since 26,280 aircraft hours multiplied by $\lambda = 15.3/100000$ failures per aircraft hour amounts to approximately 4 major loss-of-control incidents. However, as evidenced by the risk-assessment, the operation can accept such low reliability for UAS because of the area in which the operation is based. If a Reaper goes down over the specified region, it is very unlikely to strike a person or inhabited building. This result is exactly what happened when the CBP lost their first Reaper in 2006.³⁴

Table 5: Border patrol outputs.

Parameter	Value	Equivalent Representation
$F_{transient}$	6.03×10^{-9} collisions/hr	1 transient collision every 18,925 missions
F_{fleet}	1.11×10^{-7} collisions/hr	1 in-fleet collision every 1,028 missions
$F_{ped,p}$	1.35×10^{-7} strikes/hr	1 pedestrian strike due to general failure every 847 missions
$F_{ped,midair}$	2.01×10^{-11} strikes/hr	1 pedestrian strike due to midair collision every 5,682,745 missions

continued on next page...

Table 5 – Continued

Parameter	Value	Equivalent Representation
$F_{bldg,p}$	3.28×10^{-6} strikes/hr	1 building strike due to general failure every 34 missions
$F_{bldg,midair}$	3.00×10^{-10} strikes/hr	1 building strike due to midair collision every 380,478 missions
F_{ped}	1.35×10^{-7} strikes/hr	1 pedestrian strike every 847 missions
F_{bldg}	3.28×10^{-6} strikes/hr	1 building strike every 35 missions
$F_{fat,p}$	1.51×10^{-6} fatalities/hr	1 fatality due to general failure every 75 missions
$F_{fat,midair}$	2.72×10^{-7} fatalities/hr	1 fatality due to midair collisions every 420 missions
F_{fat}	1.79×10^{-6} fatalities/hr	1 fatality every 64 missions
M	17.85 dollars/hr	\$156,375 to insure per missions

B. Scenario 2: Environmental Monitoring

Environmental monitoring has been a popular non-military application for UAS in recent years. Unmanned aircraft have been used to monitor wildfires, assess damage from natural disasters, perform geomagnetic surveys, gather atmospheric data, and other environmental applications. As an example case, we will consider a team of ScanEagle UAS taking part in environmental monitoring over Northeast Washington. This risk assessment will be for wildfire detection, but the process is essentially the same for mapping,²⁵ search and rescue³⁵ or other low altitude operations.

1. UAS Properties

The wingspan, length and fuselage diameter are available³⁶ but not the propeller diameter or winglet height which must be approximated³⁷ by their size relative to known dimensions in pictures of the aircraft. Figure 7 shows how the frontal area may be approximated (the 0.3m diameter is for the propeller, which is larger than the 0.18m fuselage). The given dimensions yield an approximate area of 0.38m².

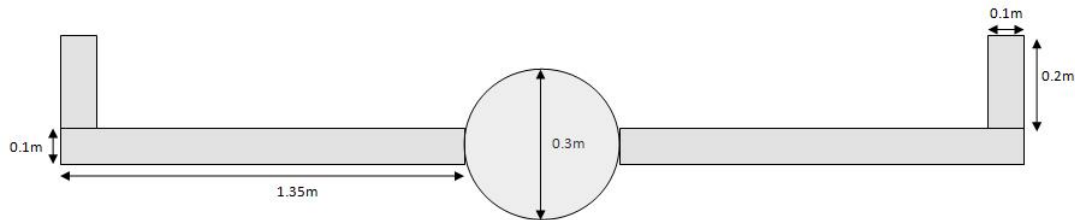


Figure 7. Frontal area approximation for ScanEagle.

A crash rate of 1 per 1,000 flight hours will be used for the calculation. Although the Navy does not officially track reliability data for the ScanEagle, loss rates have been reported between 1 in 214 flight hours and 1 in 500 flight hours.³⁸ These figures are overly pessimistic for a crash rate because they account for more than typical loss of control incidents such as damage from failed launches and recoveries or any other reason an aircraft may be deemed not airworthy.

As will be shown next section, the area of operations is spread out over two different areas. It is assumed that the team of UAS is spread out uniformly over both areas.

Working under the assumption that the path planner, whether centralized or distributed, will have knowledge of every UA's location and velocity, an in-fleet collision avoidance of 0.9 will be used. We cannot be so optimistic about ScanEagle's collision avoidance with general air traffic since reliable SAA technology is still being developed. For this reason an effectiveness of 0 will be assumed for the UA's avoidance of general air traffic. However, since ScanEagles are now equipped with ultra-light custom designed Mode C transponders, most transient aircraft will be effective in avoiding the ScanEagles. This issue will be addressed in the transient aircraft properties.

2. Operating Area

To demonstrate the tool's ability to consider multiple operating areas for a risk assessment, we will consider two areas of wildfire concern in Eastern Washington. The first is the area around Colville National Forest with its north boundary at 49°N , south boundary at 48.1°N , east boundary at 117°W and west boundary at 118.9°W . The second region will be the southeast corner of the state with its north boundary at 47°N , south boundary at 46°N , east boundary at 117°W and west boundary at 119°W .

ScanEagles typically operate around 1500ft (457m) for imaging operations,³⁹ so an altitude range of 0-1000m will be used. A generous range is chosen to include all aircraft posing a threat to the team of UA and to ensure the data returned by the automated air traffic tool is not artificially low or high. Although the ScanEagle can likely stay within several meters of a commanded altitude, looking only at air traffic in such a narrow range would not be an accurate representation. Since the automated air traffic data is based on "instantaneous" samples rather than full flight paths (which are not available), a narrow altitude range or too small of a geographic region essentially creates fickle results prone to exaggeration in either direction.

Data from the U.S. Census Bureau is used to determine the population densities by gathering the data from each zip code in the operating areas. For the Colville National Forest region, the average population density is 4.9 people/km², and the building density is 2.4 homes/km². For the Southeast Washington region, the average population density is 8.4 people/km², and the building density is 3.3 homes/km². The building densities only consider housing units, but this approximation will give an accurate model if the entire population is assigned to be an exposed pedestrian or in a housing unit. Estimating that the average person spends no more than 10% of their time outdoors, 10% of the population will be considered pedestrians, and the remaining 90% will be divided among the housing units (and accounted for in the fatalities/building-strike figure).

This estimation gives a pedestrian density of 0.49 per km² for the Colville region, and the average housing unit has 1.8 people inside. The pedestrian density for Southeast WA is 0.84 per km² with an average of 2.3 people in every building. The ScanEagle's relatively small size, light weight (around 40 lbs) and low operational speed must be taken into account when choosing the expected fatality rates. Here we will assume a pedestrian fatality rate of 50% (0.5 deaths/strike). Most homes would be effective in protecting the people inside from a ScanEagle size aircraft. Assuming the aircraft penetrates the building 10% of the time and in those cases causes the death of 10% of the people inside, the building-strike fatality rate is roughly 2×10^{-2} deaths/strike in both regions.

A team of four ScanEagles will be used in each of the operating areas over a sixth month period (the length of Washington's official wildfire season). Each UA will operate for 12 hours a day, seven days a week. The total mission length is then $6\text{months} \times 30\text{days/month} \times 12\text{hours/day} = 4320$ hours). It is assumed that the team spends a percentage of time in each operating area which is directly proportional to the size of the area. Therefore $M_L = 1949.6$ hours for the Colville National Forest operating area and $M_L = 2370.39$ hours for the Southeast Washington operating area.

3. Transient Aircraft

The transient aircraft model of these areas is obtained by tracking and recording flights using the Flight Explore over the course of one week. A more refined model may be obtained by repeating this procedure with longer sampling windows. Since the ScanEagle's typical altitude range is so low for imaging operations, any transient aircraft in the operating space will be assumed to be under the general aviation category.

Based on the historical data for the specified regions and altitude ranges, the automated air traffic tool gives an aircraft density of 7.6×10^{-7} aircraft/km² in the Colville region and 4.4×10^{-6} aircraft/km² in Southeast WA. The only remaining parameter to be filled is the transient aircraft collision avoidance. Since the ScanEagle is equipped with a Mode C transponder, general aviation's collision avoidance with the ScanEagle is expected to be on par with historical rates for the class discussed previously, which averaged 28% effectiveness.

One advantage of this formulation is that it allows the usage of multiple operating areas and multiple transient aircraft models within each operating area. The multiple operating area and transient aircraft models are shown in Table 6.

Table 6: Environmental monitoring parameters.

Parameter	Value	Comment
UAS		
V_{ua}	54 knots	-
ϕ_{ua}	0.38 m ²	-
w_{ua}	3 m	-
L_{ua}	1.5 m	-
γ	3.18 degrees	-
λ	1/1000	-
$\epsilon_{ua/o}$	0	-
$\epsilon_{ua/ua}$	0.9	-
$z_{max,fleet}$	1 km	-
$z_{min,fleet}$	0 km	-
$A_{ops,fleet}$	30803 km ²	team distributed over all operating areas
Op Area 1		Colville National Forest
N_{ua}	4	-
z_{max}	1 km	-
z_{min}	0 km	-
M_L	1949.6 hours	-
A_{ops}	13901 km ²	-
σ_b	2.4 buildings/km ²	-
A_b	200 m ²	-
H_b	5 m	-
D_{bldg}	0.018 fatalities/strike	-
σ_p	0.49 people/km ²	-
H_p	1.75 m	-
R_p	0.25 m	-
D_{ped}	0.5 fatalities/strike	50% mortality rate
Op Area 2		Southern WA
N_{ua}	4	-
z_{max}	1 km	-
z_{min}	0 km	-
M_L	2370.4 hours	-
A_{ops}	16902 km ²	-
σ_b	3.3 buildings/km ²	-
A_b	200 m ²	-
H_b	5 m	-
D_{bldg}	0.023 fatalities/strike	-
σ_p	0.84 people/km ²	-
H_p	1.75 m	-
R_p	0.25 m	-
D_{ped}	0.5 fatalities/strike	50% mortality rate
Transient AC 1		
Applied Op Area	2	Southern WA
ρ_o	4.376×10^{-6} AC/km ³	-
V_o	173 km/hr	-

continued on next page...

Table 6 – Continued

Parameter	Value	Comment
ϕ_o	22 m ²	-
P_o	3 people/AC	general aviation
ϵ_o	0.28	based on historical data
Transient AC 2		
Applied Op Area	1	Colville
ρ_o	7.604×10^{-7} AC/km ³	-
V_o	173 km/hr	-
ϕ_o	22 m ²	-
P_o	3 people/AC	general aviation
ϵ_o	0.28	based on historical data
Insurance		
I_{fat}	10,000,000 dollars/fatality	-

The input parameters for the two operating areas might be more easily visualized as pie charts as shown in Figure 8.

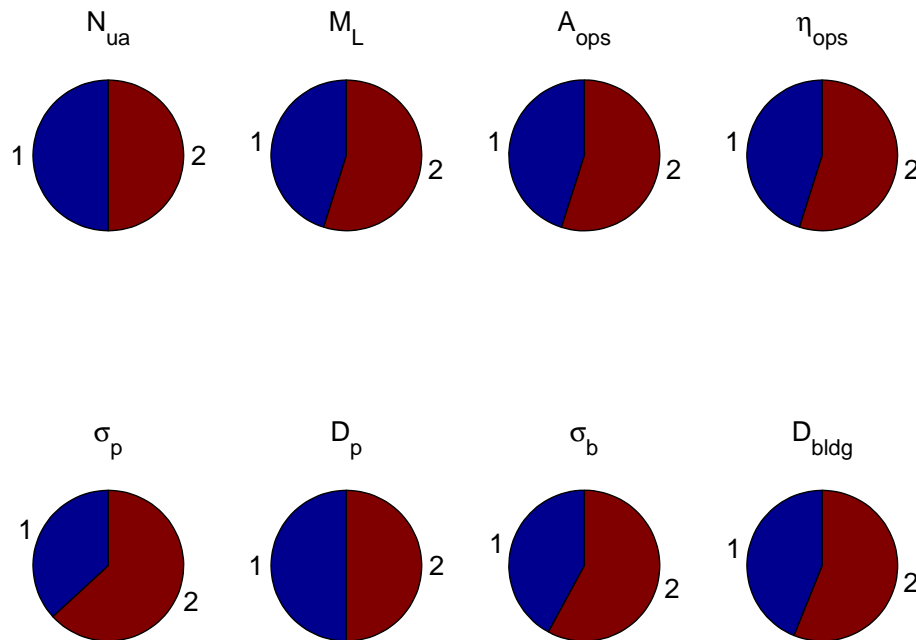


Figure 8. Input parameters for operating areas visualized as pie charts.

This shows that the team spends slightly more time in the larger, second operating area (Southeast Washington). Furthermore, the building, pedestrian density, and building fatality rate in this area is higher. One can see that this area will be the more dangerous of the two operating areas.

4. Risk Assessment Results

Because the mission is spread out over two operating areas with different transient aircraft models in each, the risk per operating area is first calculated and then combined together to provide an overall risk assessment of the entire mission. The relevant outputs are shown in Table 7.

Table 7: Environmental monitoring outputs.

Parameter	Value	Equivalent Representation
Op Area 1		
$F_{transient}$	1.68×10^{-8} collisions/hr	1 transient collision every 30,473 missions
F_{fleet}	1.18×10^{-9} collisions/hr	1 in-fleet collision every 433,078 missions
$F_{ped,p}$	2.30×10^{-7} strikes/hr	1 pedestrian strike due to general failure every 2232 missions
$F_{ped,midair}$	1.70×10^{-13} strikes/hr	1 pedestrian strike due to midair collision every 3,019,465,410 missions
$F_{bldg,p}$	1.74×10^{-5} strikes/hr	1 building strike due to general failure every 30 missions
$F_{bldg,midair}$	2.00×10^{-11} strikes/hr	1 building strike due to midair collision every 25,699,290 missions
F_{ped}	2.30×10^{-7} strikes/hr	1 pedestrian strike every 2,232 missions
F_{bldg}	1.74×10^{-5} strikes/hr	1 building strike every 30 missions
$F_{fat,p}$	4.28×10^{-7} fatalities/hr	1 fatality due to general failure every 1,199 missions
$F_{fat,midair}$	5.05×10^{-8} fatalities/hr	1 fatality due to midair collisions every 10,158 missions
F_{fat}	4.78×10^{-7} fatalities/hr	1 fatality every 1,072 missions
M	4.78 dollars/hr	\$9,325 to insure per missions
Op Area 2		
$F_{transient}$	9.69×10^{-8} collisions/hr	1 transient collision every 4,353 missions
F_{fleet}	1.18×10^{-9} collisions/hr	1 in-fleet collision every 356,198 missions
$F_{ped,p}$	3.94×10^{-7} strikes/hr	1 pedestrian strike due to general failure every 1071 missions
$F_{ped,midair}$	1.59×10^{-12} strikes/hr	1 pedestrian strike due to midair collision every 266,075,309 missions
$F_{bldg,p}$	2.40×10^{-5} strikes/hr	1 building strike due to general failure every 18 missions
$F_{bldg,midair}$	1.49×10^{-10} strikes/hr	1 building strike due to midair collision every 2,823,424 missions
F_{ped}	3.94×10^{-7} strikes/hr	1 pedestrian strike every 1,071 missions
F_{bldg}	2.39×10^{-5} strikes/hr	1 building strike every 18 missions
$F_{fat,p}$	7.47×10^{-7} fatalities/hr	1 fatality due to general failure every 565 missions
$F_{fat,midair}$	2.91×10^{-7} fatalities/hr	1 fatality due to midair collisions every 1,451 missions
F_{fat}	1.04×10^{-6} fatalities/hr	1 fatality every 407 missions
M	10.37 dollars/hr	\$24,592 to insure per missions
Total		
$F_{transient}$	6.08×10^{-8} collisions/hr	1 transient collision every 3,809 missions
F_{fleet}	1.18×10^{-9} collisions/hr	1 in-fleet collision every 195,447 missions
$F_{ped,p}$	3.20×10^{-7} strikes/hr	1 pedestrian strike due to general failure every 724 missions
$F_{ped,midair}$	9.47×10^{-13} strikes/hr	1 pedestrian strike due to midair collision every 244,527,541 missions
$F_{bldg,p}$	2.10×10^{-5} strikes/hr	1 building strike due to general failure every 11 missions
$F_{bldg,midair}$	9.10×10^{-11} strikes/hr	1 building strike due to midair collision every 2,543,937 missions
F_{ped}	3.20×10^{-7} strikes/hr	1 pedestrian strike every 724 missions
F_{bldg}	2.10×10^{-5} strikes/hr	1 building strike every 11 missions
$F_{fat,p}$	6.03×10^{-7} fatalities/hr	1 fatality due to general failure every 384 missions
$F_{fat,midair}$	1.82×10^{-7} fatalities/hr	1 fatality due to midair collisions every 1,270 missions
F_{fat}	7.85×10^{-7} fatalities/hr	1 fatality every 295 missions
M	7.85 dollars/hr	\$33,917 to insure per missions

For the Colville National Forest region (operating area 1), the predicted transient midair collision rate dominates over the in-fleet collision rate (1.68×10^{-8} vs. 1.18×10^{-9}) which may be attributed to the effective in-fleet collision avoidance of $\epsilon_{ua/ua} = 0.9$. We still observe that major hazard to human life is still general system failures rather than midair collisions (1 fatality due to system failures every 1,199 missions vs. 1 fatality due to midair collisions every 10,158 missions). If every fatality is covered by a \$10 million insurance policy, the price to insure the operation is \$4.78 per hour which gives a mission cost of \$9,325 for the team of four ScanEagles in this operating area. Also note that the total fatality rate is higher rate than the pedestrian strike rate. This is due to the relatively high building strike rate and associated fatalities from building strikes (which are not included as pedestrian fatalities).

As expected, operations over the Southeast Washington operating area (operating area 2) are more risky. For a single mission, the expected number of fatalities is 0.0024592 vs. 0.00093252 (almost 3 times more fatalities expected in this area). This can be attributed to the fact that the team spends more time in this more densely populated region. The cost to insure the mission in this region amounts to \$24,592 per mission.

For the total mission spread out over both operating areas, it is expected that 1 fatality will occur every 295 missions. Assuming 1 mission is flown each year during the wildfire season, this is equivalent to 1 fatality every 295 years.

The inherent relative danger between the two operating areas can be more easily visualized as pie charts as shown in Figure 9.

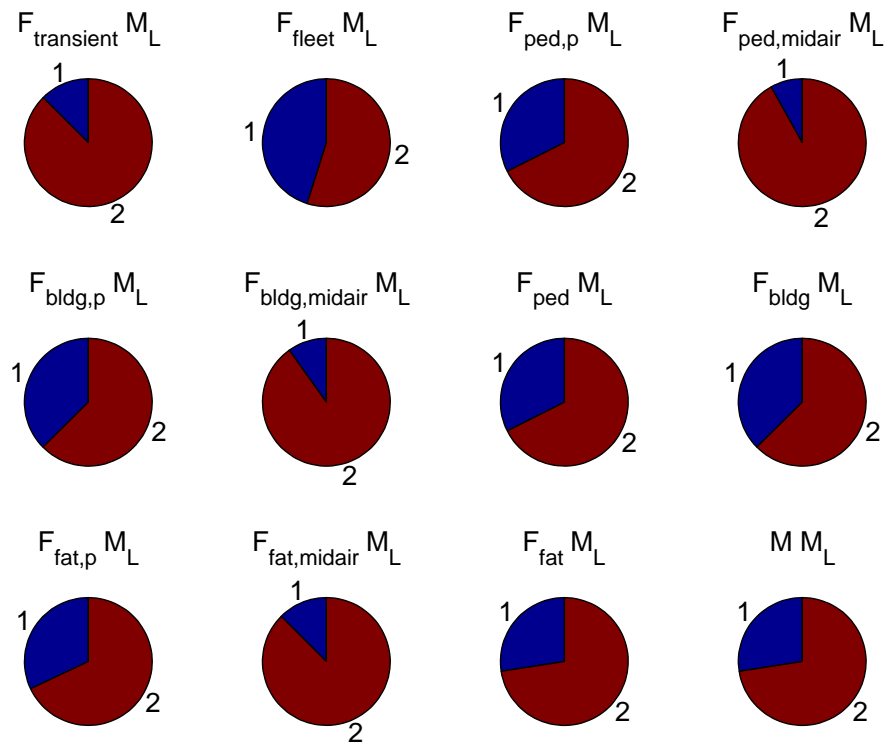


Figure 9. Output parameters for operating areas visualized as pie charts. Quantities are total occurrences in each operating area (ie row 1, column 1 represents total number of transient collisions in each operating area)

As can be seen from Figure 9, operating area 2 is more dangerous in almost every quantity. The only quantity where there are a similar number of occurrences is the number of in-fleet collisions (row 1, column 2). In other areas such as the number of building strikes due to midair collisions (row 2, column 2), operating area 2 is clearly more dangerous. In the end, it can be seen that nearly 3/4 of the number of fatalities and

required insurance costs (row 3, columns 3 and 4 respectively) are attributed to operations over operating area 2. If operations could be contained solely within the Colville Nation Forest region, fatalities and insurance costs would dramatically decrease.

C. Scenario 3: Urban Patrol

The previous two examples represented the type of operations for which UAS are feasible near term solutions. The following example will demonstrate why many other suggested uses for UAS are expected to be less viable in the near term from the perspectives of safety and economics. While they may have technical merit and excellent potential benefits, risk analysis reveals significant safety issues that will prevent regulatory approval and public acceptance. One such application is the use of UAS to patrol urban environments to provide traffic monitoring, law enforcement surveillance, anti-terrorist intelligence, and other services. The idea is that a group of UAS can be used to provide persistent surveillance over a high value target such as a city and monitor areas of interests such as harbors, airports, highways, and other avenues of ingress and egress. This application has been proposed by individuals in academia^{40,41} and explored by some governmental agencies.⁴² This scenario will serve as a final sample case.

1. UAS Properties

Several case studies and trials have selected MLB's BAT 3 for traffic monitoring projects, so its specifications will be used here in this urban patrol scenario. The manufacturer lists the BAT 3's speed as 35-60 knots, so an operational speed of 50 knots will be assumed. The aircraft has a 6ft wingspan, 4.7ft length and 2ft height. Since no dimensioned drawings are available, the frontal area will be conservatively approximated as a 6ft×2ft rectangle giving an area of 12ft².

Data is not published on the BAT 3's glide angle or failure rate, although a group operating the aircraft would either have this information or determine it during testing. We will assume a lift to drag ratio of 15:1 which yields a glide angle of $\tan^{-1}(1/15) = 3.8^\circ$. A failure rate of one mishap per 1,000 flight hours, representative of this class of UAS, will be assumed. The BAT 3 does not have collision avoidance ability with non-cooperative aircraft, aside from the pilot's ability to see and avoid using onboard cameras, so a general collision avoidance of 0 will be used. Knowing the position of other traffic monitoring UA should allow very effective in-fleet collision avoidance, so a value of 0.9 will be assumed.

2. Operating Area

The city of Seattle, Washington in the United States will be used as an example city. This city is unique because it borders the Puget Sound, a large body of water and major maritime shipping environment. The total operating area will be broken into two smaller operating areas. The first will represent the land based environments and the second operating area will be representative of the marine environments. These areas are shown in Figure 10. This example shows that the operating areas do not need to be perfect rectangles. Irregularly shaped areas can be approximated by rectangles of equivalent area. Some image processing using reference shapes of known area yields 637.27 km² of land and 333.6 km² of water in this area.

As depicted in Figure 10, the area being considered will include several major suburbs of Seattle as well as major port and shipping lanes of the Puget Sound region. To cover this area, it is assumed that 4 UAS are dedicated to patrolling the total area 24 hours a day, 7 days a week, for 1 year. Similar to example 2, the time spent in each operating area is directly proportional to the area, yielding $M_L = 4750$ hours for operating area 1 and $M_L = 3010$ hours for operating area 2. The team will be operated in an altitude range of 500ft to 3000ft.

For operating area 1, population figures will be based on global data for the 981XX area codes. This region does not match up exactly with the area shown in Figure 10, but the data will provide a good approximation. According to the U.S. Census Bureau, the 981XX area codes average 2,767 people/mi² and 1,270 housing units/mi². As in the previous two examples, the simplest way to model the population is to assume everyone is either outside (pedestrian) or in a housing unit. Since the region being modeled is very urban, 15% of the population will be assumed to be outside (10% was used in other example calculations) which gives a pedestrian density of 415/mi². Dividing the remaining population evenly between the housing units results in 1.9 people inside the average housing unit. To account for larger industrial buildings, the average structure size is slightly larger than the two previous examples. An average structure size of 2,500ft²

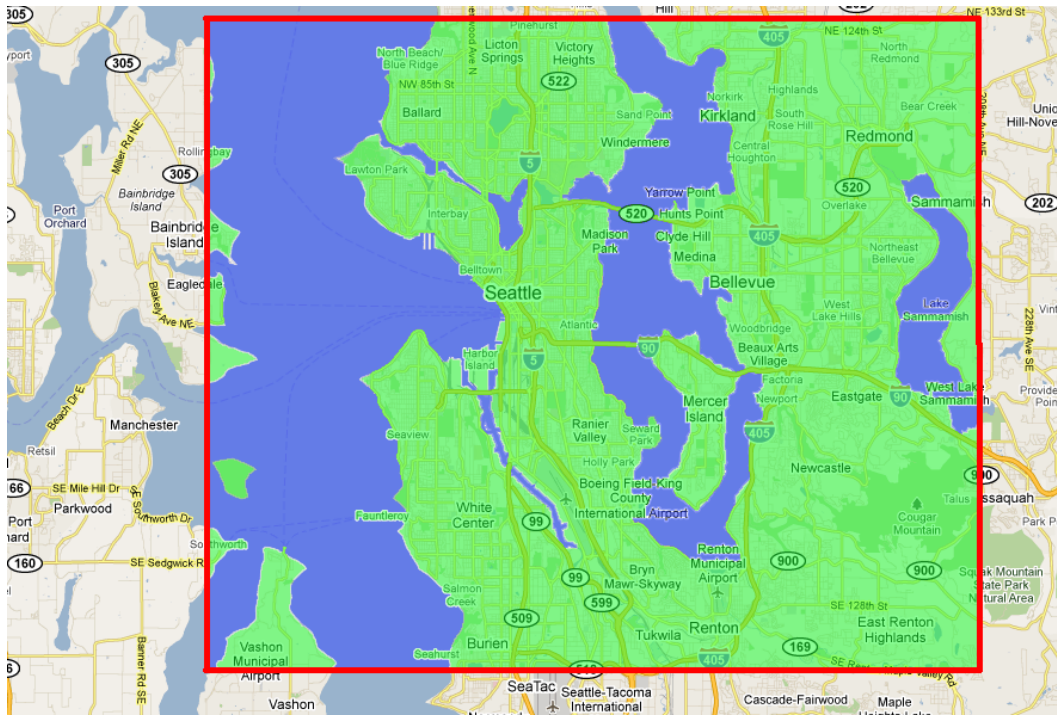


Figure 10. Operating area 1 (urban environments) shown in light green and operating area 2 (marine environments) shown in bright blue. Red box denotes total patrol area for UAS team.

and 30ft high will be used. Given the small size and weight (25 lbs) of the BAT 3, only 10% of aircraft that strike a building will be assumed to penetrate the structure, resulting in the death of 10% of the people inside. This estimation gives an average of 2×10^{-2} fatalities per building strike. For pedestrians a fatality rate of 75% will be assumed given the characteristics of the UA.

For operating area 2, the only human population in this environment is those aboard ships and boats and the occasional swimmer. The ships in this region will be modeled as buildings. Ship population in this region is comprised ferries, commercial shipping vessels, and private pleasure craft. Averaging estimates of vessel numbers, populations, and dimensions yields a density of $\sigma_b = 0.42$ vessels/km², $A_b = 116$ m², and $H_b = 4.6$ m. The average population on each ship is estimated to be 23 persons/vessel. Assuming that a ship is more vulnerable than a building, we assume that a strike will result in the death of 25% of the people, yielding $D_{bldg} = 5.8$ fatalities per strike. Assuming that there are 200 people swimming at any point in time, we have $\sigma_p = 0.59$ people/km². We can model these as swimmers instead of standing individuals by modifying H_p and R_p . Furthermore, we assume $D_{ped} = 0.9$ to model the fact that striking a swimmer is highly likely to result in a fatality.

3. Transient Aircraft

The air traffic densities are computed from the database described previously. Typically, at this low altitude range one would assume that the majority of air traffic is from general aviation. However, since the operation is taking place near several airports, the default distribution (37% commercial jets, 30% regional jets, 33% general aviation) will still be used to model the air traffic.

The FAA will undoubtedly require any UAS operating so near a major airport to be equipped with transponders regardless of their operating altitude. Commercial and regional jets, which are equipped with TCAS, will then have the ability to reliably avoid a midair collision with the BAT 3. Collision avoidance should be conservative, however, since the BAT 3's small size will limit the ability of a transient aircraft pilot to see and avoid the aircraft. Collision avoidance of 80% will be assumed for commercial and regional jets and 20% for general aviation.

The input parameters for this calculation are shown in Table 8.

Table 8: Urban patrol parameters.

Parameter	Value	Comment
UAS		
V_{ua}	50 knots	-
ϕ_{ua}	0.11 m ²	-
w_{ua}	6 ft	-
L_{ua}	4.7 ft	-
γ	3.18 degrees	-
λ	1/1000	-
$\epsilon_{ua/o}$	0	-
$\epsilon_{ua/ua}$	0.9	-
$z_{max,fleet}$	3000 ft	-
$z_{min,fleet}$	500 ft	-
$A_{ops,fleet}$	970.9 km ²	team distributed over all operating areas
Op Area 1		Land environments
N_{ua}	4	-
z_{max}	3000 ft	-
z_{min}	500 ft	-
M_L	5750 hours	-
A_{ops}	637 km ²	-
σ_b	1270 buildings/mi ²	-
A_b	2500 ft ²	-
H_b	30	-
D_{bldg}	0.02 fatalities/strike	-
σ_p	415 people/mi ²	-
H_p	1.75 m	-
R_p	0.25 m	-
D_{ped}	0.75 fatalities/strike	75% mortality rate
Op Area 2		Water environments
N_{ua}	4	-
z_{max}	3000 ft	-
z_{min}	500 ft	-
M_L	3010 hours	-
A_{ops}	333.6 km ²	-
σ_b	0.42 buildings/km ²	vessels modeled as buildings
A_b	116 m ²	-
H_b	4.6 m	-
D_{bldg}	5.76 fatalities/strike	-
σ_p	0.60 people/km ²	-
H_p	.25 m	swimmer height
R_p	1 m	swimmer length
D_{ped}	0.9 fatalities/strike	high mortality rate
Transient AC 1		Commercial flights
Applied Op Area	1, 2	applies to both areas
ρ_o	1.033×10^{-6} AC/km ³	-
V_o	437 knots	-

continued on next page...

Table 8 – Continued

Parameter	Value	Comment
ϕ_o	175 m ²	-
P_o	175 people/AC	-
ϵ_o	0.8	under ATC guidance
Transient AC 2 Applied Op Area	1, 2	Regional jets applies to both areas
ρ_o	9.217×10^{-7} AC/km ³	-
V_o	432 knots	-
ϕ_o	80 m ²	-
P_o	45 people/AC	-
ϵ_o	0.8	under ATC guidance
Transient AC 3 Applied Op Area	1, 2	General aviation applies to both areas
ρ_o	8.379×10^{-7} AC/km ³	-
V_o	173 knots	-
ϕ_o	22 m ²	-
P_o	3 people/AC	-
ϵ_o	0.2	historical see and avoid
Insurance I_{fat}	10,000,000 dollars/fatality	-

4. Risk Assessment Results

The results of this risk assessment are summarized in Table 9.

Table 9: Urban patrol outputs.

Parameter	Value	Equivalent Representation
Op Area 1		
$F_{transient}$	2.54×10^{-7} collisions/hr	1 transient collision every 683 missions
F_{fleet}	4.01×10^{-7} collisions/hr	1 in-fleet collision every 432 missions
$F_{ped,p}$	0.0001 strikes/hr	1 pedestrian strike due to general failure every 1.3 missions
$F_{ped,midair}$	8.92×10^{-10} strikes/hr	1 pedestrian strike due to midair collision every 194,957 missions
$F_{bldg,p}$	0.0154 strikes/hr	1 building strike due to general failure every 0.01 missions
$F_{bldg,midair}$	1.46×10^{-7} strikes/hr	1 building strike due to midair collision every 1,185 missions
F_{ped}	0.0001 strikes/hr	1 pedestrian strike every 1.3 missions
F_{bldg}	0.015 strikes/hr	1 building strike every 0.01 missions
$F_{fat,p}$	0.0004 fatalities/hr	1 fatality due to general failure every 0.4 missions
$F_{fat,midair}$	2.97×10^{-5} fatalities/hr	1 fatality due to midair collisions every 5.8 missions
F_{fat}	0.0004 fatalities/hr	1 fatality every 0.4 missions
M	4,329 dollars/hr	\$24,892,721 to insure per missions
Op Area 2		
$F_{transient}$	2.54×10^{-7} collisions/hr	1 transient collision every 1,305 missions
F_{fleet}	4.01×10^{-7} collisions/hr	1 in-fleet collision every 826 missions
$F_{ped,p}$	1.98×10^{-7} strikes/hr	1 swimmer strike due to general failure every 1,675 missions

continued on next page...

Table 9 – Continued

Parameter	Value	Equivalent Representation
$F_{ped,midair}$	9.06×10^{-12} strikes/hr	1 swimmer strike due to midair collision every 36,660,342 missions
$F_{bldg,p}$	7.89×10^{-7} strikes/hr	1 vessel strike due to general failure every 420 missions
$F_{bldg,midair}$	6.96×10^{-11} strikes/hr	1 vessel strike due to midair collision every 4,767,893 missions
F_{ped}	1.98×10^{-7} strikes/hr	1 swimmer strike every 1,675 missions
F_{bldg}	7.89×10^{-7} strikes/hr	1 vessel strike every 420 missions
$F_{fat,p}$	4.73×10^{-6} fatalities/hr	1 fatality due to general failure every 70 missions
$F_{fat,midair}$	2.96×10^{-5} fatalities/hr	1 fatality due to midair collisions every 11 missions
F_{fat}	3.44×10^{-5} fatalities/hr	1 fatality every 9 missions
M	344.31 dollars/hr	\$1,036,401 to insure per missions
Total		
$F_{transient}$	2.54×10^{-7} collisions/hr	1 transient collision every 448 missions
F_{fleet}	4.01×10^{-7} collisions/hr	1 in-fleet collision every 284 missions
$F_{ped,p}$	8.28×10^{-5} strikes/hr	1 pedestrian strike due to general failure every 1.3 missions
$F_{ped,midair}$	5.88×10^{-10} strikes/hr	1 pedestrian strike due to midair collision every 193,926 missions
$F_{bldg,p}$	0.01 strikes/hr	1 building strike due to general failure every 0.01 missions
$F_{bldg,midair}$	9.62×10^{-8} strikes/hr	1 building strike due to midair collision every 1,185 missions
F_{ped}	8.28×10^{-5} strikes/hr	1 pedestrian strike every 1.4 missions
F_{bldg}	0.01 strikes/hr	1 building strike every 0.01 missions
$F_{fat,p}$	0.0002 fatalities/hr	1 fatality due to general failure every 0.43 missions
$F_{fat,midair}$	2.97×10^{-5} fatalities/hr	1 fatality due to midair collisions every 3.8 missions
F_{fat}	0.0003 fatalities/hr	1 fatality every 0.4 missions
M	2959.94 dollars/hr	\$25,929,123 to insure per missions

The most striking result of this analysis is the high level of risk this operation incurs. Due to the high density of people and buildings, both pedestrian and building strikes are virtually guaranteed over the course of a mission/year. In total, there are over 2 fatalities expected each mission/year. This leads to over \$25 million dollars per mission/year to adequately cover this operation.

Once again we see that the cause of these fatalities are mostly due to the unreliability of the UAS rather than midair collisions ($F_{fat,p} \approx 9F_{fat,midair}$).

The relative risk incurred with respect to each operating area can be compared as shown in Figure 11.

As expected, the majority of the risk originates from operation area 1 (land environments). Flying missions over densely populated areas is not an inherently safe operation. Only 4.2% of the fatalities are caused by maritime accidents. Note that although this may seem like a small amount relative to the fatalities on land, in absolute terms, there are still an expected 0.1 maritime fatalities per mission/year (and costing over \$1 million dollars to insure against maritime fatalities).

These costs clearly indicate that using UAS to patrol in an urban environment context is not currently a safe or economically viable option. These expenses represent only the insurance risk from human safety, not UAS repair and replacement costs, property damage, and other general operational costs. Given the present state of UAS, other options such as manned aircraft or ground-based cameras are likely better options from financial and safety points of view.

VII. Conclusions and Further Research

The risk assessment tool presented in this paper is designed to be a reliable, accurate, and easily accessible method to estimate the risk to human life incurred from a given UAS operation. This model does not take into account economic factors such as costs of replacing UAS and structural damage caused by building strikes. The human safety factor is expressed in economic terms based on a user-specified liability protection

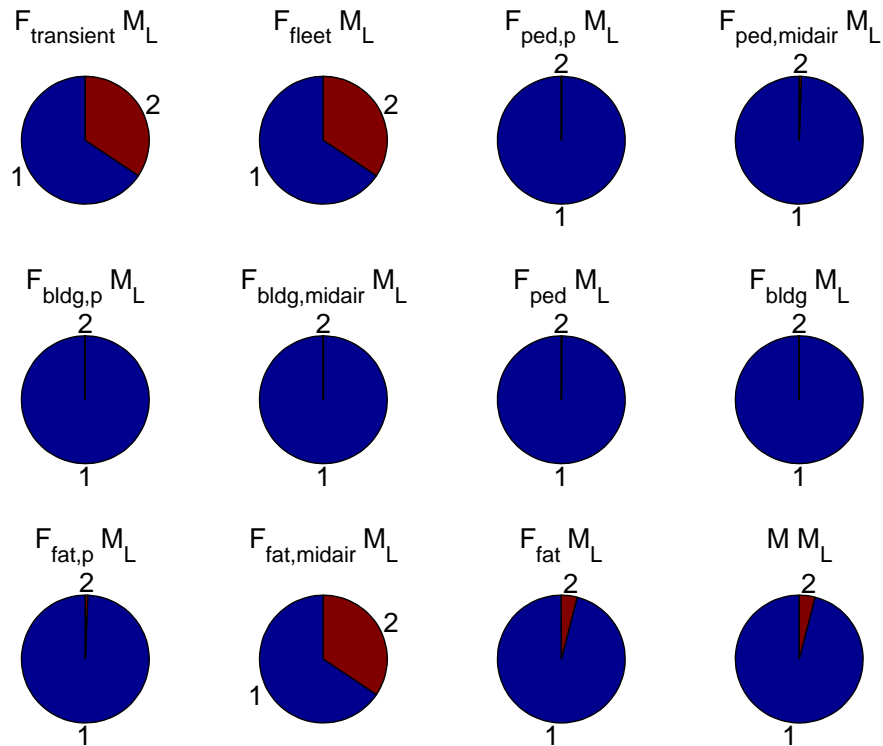


Figure 11. Output parameters for operating areas visualized as pie charts. Quantities are total occurrences in each operating area (ie row 1, column 1 represents total number of transient collisions in each operating area).

per fatality. This cost serves to give the user a tangible measure of the risk, since a cost per hour is often times easier to grasp than the expected number of fatalities per hour.

A risk assessment is currently limited to a single UAS model for the entire operation. The tool can be given even greater flexibility by allowing the calculation to accommodate multiple UAS models within a single operation. This feature would allow an operation that uses a team of heterogeneous UA to be represented more accurately. The user could also be given more freedom by having the option to calculate the required level of UAS reliability to meet a specified level of risk. Other variables, such as air traffic and population densities, could also be determined in place of the safety risk, which is useful in selecting an appropriate operating area.

At this early point in the domestic deployment of UAS, one can assume most UAS operations will not be near busy highways and roads. However, one purpose of this tool is to predict the risk of potential future operations in order to encourage the safe expansion of UAS utilization. Since many useful operations can be imagined in which UAS operate near or directly over automobile traffic, the operating area properties could be expanded to include information on roads and traffic in the region. One would simply treat the expected number of vehicles as small buildings in the current model, but this solution is less than ideal. In a similar fashion, the transient aircraft models could be expanded to include structured airways, jetways, and other regions of abnormally high aircraft density.

Currently, the most difficult parameter to obtain is the density of the transient aircraft. Current estimates are obtained by sampling over a small, desired region to build a small database. Expanding the air traffic database is a simple way to significantly improve the tool's usefulness. Hopefully, automated air traffic data will eventually be available for the entire NAS. In addition to increasing the area covered, the depth of the historical data also needs to be improved. With a larger sampling of air traffic, additional filters can be used to improve the model's accuracy by matching items such as time of day, season/month of year and day of the week. Presently, the user must modify the default air traffic distribution between aircraft type based on

the altitude range and their knowledge of traffic through the airspace. The raw data being gathered actually has the information necessary to assign 90% or more of the traffic to one of the transient aircraft models. The aircraft codes used by the data provider must be assigned to one of the three aircraft models so that the sorting algorithm is able to distinguish between type of aircraft and automatically set the distribution.

As is the case with most numerical models, the results and output of the model are highly dependent on the accuracy of the inputs. Based on perturbation analysis, it appears that the easiest way to reduce expected fatalities and injuries is to improve UAS reliability (increase λ). The majority of fatalities can be traced back to a general UAS system failure. Many of the examples presented in this work become significantly more attractive from a safety standpoint if a less conservative value of λ is used. This result is reassuring because for the near future, this is the parameter that is most easily influenced by new technologies and engineering analysis.

VIII. Acknowledgements

The work reported here was sponsored in part by AFOSR SBIR FA8501-10-P-9005. Juris Vagners (Professor Emeritus, Dept. of Aeronautics and Astronautics, vagners@aa.washington.edu), Tad McGeer (Founder, Aerovel, tad@aerovelco.com), Jonas Michael, and Timothy Lum contributed to this paper.

References

- ¹Anno, J., "Estimate of Human Control Over Mid-Air Collisions," *Journal of Aircraft*, Vol. 19, No. 1, 1982, pp. 86–88.
- ²Burke, D., *System Level Airworthiness Tool: A Comprehensive Approach to Small Unmanned Aircraft System Airworthiness*, Ph.D. thesis, North Carolina State University, 2010.
- ³McGraw, J., "AFS-400 UAS Policy 05-01, Unmanned Aircraft Systems Operations in the U.S. National Airspace System - Interim Operational Approval Guidance," Federal Aviation Administration.
- ⁴Sabatini, N., "Unmanned Aircraft Operations in the National Airspace System," Federal Aviation Administration.
- ⁵Davis, K., "Interim Operational Approval Guidance 08-01, Unmanned Aircraft Systems Operations in the U.S. National Airspace System," Federal Aviation Administration.
- ⁶Paskiewicz, F., "Order 8130.34: Airworthiness Certification of Unmanned Aircraft Systems," Federal Aviation Administration.
- ⁷Vuren, R. V., "Advisory Circular 91-57: Model Aircraft Operating Standards," Federal Aviation Administration.
- ⁸"STANAG 4671 Unmanned Aerial Vehicle Systems Airworthiness Requirements (USAR)," NATO Document, Sept. 2009.
- ⁹"Policy Statement Airworthiness Certification of Unmanned Aircraft Systems (UAS)," European Aviation Safety Agency (EASA), Aug. 2009.
- ¹⁰"FAA's NextGen Implementation Plan," Federal Aviation Administration.
- ¹¹F. Martel, R.R. Schultz, W.H. Semke, Z. Wang, and M. Czarnomski, "Unmanned Aircraft Systems Sense and Avoid Avionics Utilizing ADS-B Transceiver," April 2009.
- ¹²A. Lacher, A. Zeitlin, D. Maroney, K. Markin, D. Ludwig, and J. Boyd, "Airspace Integration Alternatives for Unmanned Aircraft," CAASD, The MITRE Corporation, Feb. 2010.
- ¹³"SAA Workshop Final Report: Sense and Avoid for Unmanned Aircraft Systems," Federal Aviation Administration.
- ¹⁴McGeer, T., "Safety, Economy, Reliability, And Regulatory Policy For Unmanned Aircraft," Aerovel Corporation.
- ¹⁵"United States Air Force Class A Aerospace Mishaps," Accident Investigation Board.
- ¹⁶"Aircraft Statistics- Flight Mishap Histories," Air Force Safety Center.
- ¹⁷Herz, R., *Assessing the Influence of Human Factors and Experience on Predator Mishaps*, Ph.D. thesis, Northcentral University, 2008.
- ¹⁸R. Nullmeyer, R. Herz, and G. Montijo, "Training Interventions to Reduce Air Force Predator Mishaps," Air Force Research Laboratory, April 2009.
- ¹⁹R.A. Dolbeer, S.E. Wright, J. Weller, and M.J. Begier, "Wildlife Strikes to Civil Aircraft in the United States 1990-2008," Animal and Plant Health Inspection Service and Federal Aviation Administration.
- ²⁰McQuarrie, D. and Simon, J., "Physical Chemistry: A Molecular Approach," .
- ²¹McGeer, T., Newcome, L., and Vagners, J., "Quantitative Risk Management as a Regulatory Approach to Civil UAVs," .
- ²²McGeer, T., "Aerosonde Hazard Estimation," Aerovel Corporation.
- ²³Schmidt, M. and Lipson, H., "Distilling Free-Form Natural Laws from Experimental Data," *Science*, April 1958, pp. 81–85.
- ²⁴Lum, C. W., Vagners, J., Jang, J. S., and Vian, J., "Partitioned Searching and Deconfliction: Analysis and Flight Tests," *Proceedings of the 2010 American Control Conference*, Baltimore, MD, June 2010.
- ²⁵Lum, C. W., Rysdyk, R. T., and Pongpunwattana, A., "Autonomous Airborne Geomagnetic Surveying and Target Identification," *Proceedings of the 2005 Infotech@Aerospace Conference*, AIAA, Arlington, VA, September 2005.
- ²⁶Lum, C. W., *Coordinated Searching and Target Identification Using Teams of Autonomous Agents*, Ph.D. thesis, University of Washington, Seattle, WA, March 2009.

- ²⁷Klein, D. J., *Coordinated Control and Estimation for Multi-agent Systems: Theory and Practice*, Ph.D. thesis, University of Washington, Seattle, WA, September 2008.
- ²⁸R. Clothier, R. Walker, N. Fulton, and D. Campbell, "A Casualty Risk Analysis For Unmanned Aerial System (UAS) Operations Over Inhabited Areas," Twelfth Australian International Aerospace Congress, March 2007.
- ²⁹"Range Safety Criteria For Unmanned Air Vehicles," Tech. rep., Range Safety Group and Range Commanders Council, US Army White Sands Missile Range, New Mexico 88002-5110, 2007.
- ³⁰Customs and Agency, B. P., "U.S. Customs and Border Protection UAS Overview," Feb. 2009.
- ³¹Eaton, T., "Unmanned planes could begin flying over Texas in a matter of months," may 2010.
- ³²Atomics, G., "Predator B Persistent Multi-Mission ISR," May 2009.
- ³³Center, A. F. S., "MQ-9 UAS Mishap History," Dec. 2009.
- ³⁴Board, N. T. S., "NTSB Identification: CHI06MA121," Oct. 2007, Accident report.
- ³⁵Lum, C. W. and Vagners, J., "A Modular Algorithm for Exhaustive Map Searching Using Occupancy Based Maps," *Proceedings of the 2009 Infotech@Aerospace Conference*, Seattle, WA, April 2009.
- ³⁶Insitu, "ScanEagle Data Sheet," Oct. 2009.
- ³⁷Naval-Technology.com, "ScanEagle Mni-UAV Specifications," .
- ³⁸Clingan, B., "FY 2008 Navy UAS, UCAS and EPX Programs," March 2007, Statement before the Tactical Air and Land Forces Subcommittee.
- ³⁹Frontiers, B., "ScanEagle supports rescue of freighter captain held by pirates," April 2009.
- ⁴⁰B. Coifman, M. McCord, R.G. Mishalani, M. Iswalt, and Y. Ji, "Roadway traffic monitoring from an unmanned aerial vehicle," IEE Proceedings, March 2006.
- ⁴¹K. Ro, J. Oh, and L. Dong, "Lessons Learned: Application of Small UAV for Urban Highway Traffic Monitoring," AIAA Aerospace Sciences Meeting and Exhibit, Jan. 2007.
- ⁴²McCormack, E., "The Use of Small Unmanned Aircraft by the Washington state Department of Transportation," .